

NBER WORKING PAPER SERIES

THE INTERGENERATIONAL MORTALITY TRADEOFF OF COVID-19 LOCKDOWN
POLICIES

Lin Ma
Gil Shapira
Damien de Walque
Quy-Toan Do
Jed Friedman
Andrei A. Levchenko

Working Paper 28925
<http://www.nber.org/papers/w28925>

NATIONAL BUREAU OF ECONOMIC RESEARCH
1050 Massachusetts Avenue
Cambridge, MA 02138
June 2021

We are grateful to Mohamed Abdel Jelil, Jishnu Das, Shanta Devarajan, Xavier Devictor, Rema Hanna, Aaditya Mattoo, Mushfiq Mobarak and Nina Yamanis for helpful comments. The findings, interpretations, and conclusions expressed in this work do not necessarily reflect the views of the World Bank, its Board of Executive Directors, or the governments they represent. The World Bank does not guarantee the accuracy of the data included in this work. The views expressed herein are those of the authors and do not necessarily reflect the views of the National Bureau of Economic Research.

NBER working papers are circulated for discussion and comment purposes. They have not been peer-reviewed or been subject to the review by the NBER Board of Directors that accompanies official NBER publications.

© 2021 by Lin Ma, Gil Shapira, Damien de Walque, Quy-Toan Do, Jed Friedman, and Andrei A. Levchenko. All rights reserved. Short sections of text, not to exceed two paragraphs, may be quoted without explicit permission provided that full credit, including © notice, is given to the source.

The Intergenerational Mortality Tradeoff of COVID-19 Lockdown Policies

Lin Ma, Gil Shapira, Damien de Walque, Quy-Toan Do, Jed Friedman, and Andrei A. Levchenko
NBER Working Paper No. 28925

June 2021

JEL No. I15,I18

ABSTRACT

In lower-income countries, the economic contractions that accompany lockdowns to contain the spread of COVID-19 can increase child mortality, counteracting the mortality reductions achieved by the lockdown. To formalize and quantify this effect, we build a macro-susceptible-infected-recovered model that features heterogeneous agents and a country-group-specific relationship between economic downturns and child mortality, and calibrate it to data for 85 countries across all income levels. We find that in low-income countries, a lockdown can potentially lead to 1.76 children's lives lost due to the economic contraction per COVID-19 fatality averted. The ratio stands at 0.59 and 0.06 in lower-middle and upper-middle income countries, respectively. As a result, in some countries lockdowns actually can produce net increases in mortality. The optimal lockdowns are shorter and milder in poorer countries than in rich ones, and never produce a net mortality increase.

Lin Ma
AS2 #05-19
National University of Singapore
Singapore
ecsml@nus.edu.sg

Quy-Toan Do
The World Bank
1818 H Street NW
Washington, DC 20433
qdo@worldbank.org

Gil Shapira
The World Bank
1818 H street, NW
Washington, DC 20433
gshapira@worldbank.org

Jed Friedman
The World Bank
1818 H street, NW
Washington, DC 20433
jfriedman@worldbank.org

Damien de Walque
The World Bank
Development Research Group
1818 H Street, NW
Washington, DC 20433
ddewalque@worldbank.org

Andrei A. Levchenko
Department of Economics
University of Michigan
611 Tappan Street
Ann Arbor, MI 48109
and CEPR
and also NBER
alev@umich.edu

1 Introduction

Governments across the world introduced unprecedented lockdown policies in an attempt to contain the spread of COVID-19. Unsurprisingly, a debate soon erupted on what type of lockdowns were warranted and whether the benefits of such policies justify the accompanying dramatic economic contractions. Embracing utilitarianism, economists, among others, focused on the tradeoff between the lives saved by a lockdown and its economic costs (Hall et al., 2020; Kim and Loayza, 2021). On the other hand, both proponents of deontological ethics and critics of the statistical value of life recused a policy analytic approach that involves the monetary valuation of life (Singer and Plant, 2020; Viscusi and Aldy, 2003; Slovic and Peters, 2006). This paper casts a new light on this debate by bringing to light an intergenerational mortality tradeoff inherent to pandemic mitigation as the disease and the lockdown policies affect the mortality of younger and older individuals differentially.

In the early days of the pandemic, evidence emerged that the COVID-19 mortality risk increases substantially with age (Verity et al., 2020). Heterogeneous age profiles of mortality risk are in fact common in epidemics, and were also present in the 1918-1919 influenza pandemic and in two recent emergent diseases – Severe Acute Respiratory Syndrome (SARS) and Ebola – which induced sustained pandemic concern in the global community.¹ On the other hand, previous research has shown that infant and child mortality in low- and middle-income countries is counter-cyclical (Pritchett and Summers, 1996; Bhalotra, 2010; Baird et al., 2011; Cruces et al., 2012; Friedman and Schady, 2013). This implies that lockdown policies in developing countries can lead to an increase in infant and child mortality due to the consequent economic contraction. Thus, pandemic mitigation policies in low-income settings not only forgo economic well-being to save lives but also embed a tradeoff between one life and another.

This paper quantitatively evaluates this tradeoff in a Susceptible-Infected-Recovered

¹The 1918-19 influenza pandemic was characterized by an age shift with most excess deaths occurring among young adults (ages 15-44) and fewer excess deaths occurring among those over 65 (Olson et al., 2005; Andreasen et al., 2008). The Ebola case fatality rates for young children under 5 and for elders over 75 are both approximately 80 percent higher than for prime-age adults (Garske et al., 2017). During the 2003 SARS outbreak, the case fatality rate was estimated to be an order of magnitude higher for patients in China over 60 years of age than those under 40 years (25 percent vs 2 percent) (Jia et al., 2009). A similar age gradient was observed in Hong Kong during the same outbreak (Karlberg et al., 2004).

(SIR)-macro model (e.g. [Eichenbaum et al., 2020](#)) augmented with two main features. First, a lockdown can potentially increase child mortality by inducing an economic contraction. The main innovation of our paper is to model and quantify this effect. We estimate country-group-specific semi-elasticities of child mortality with respect to aggregate income by applying the methodology of [Baird et al. \(2011\)](#) to microdata from 83 countries, and use the resulting estimates in our quantitative model. Second, to capture the key mechanism we relax the representative agent assumption of most SIR-macro models and allow for several types of agents that differ by age. Our economy comprises of young, adult, and elderly members (as in [Acemoglu et al., 2020](#)).

Infection is assumed to spread through work, consumption-related activities, and community and intra-household interactions. Adults are the only ones supplying labor, trading consumption off against the risk to themselves and their relatives of contracting COVID-19. A decentralized equilibrium is characterized by excess supply of labor since individuals do not internalize the social cost of being infected, which consists of an increased probability of infection for all susceptible individuals as well as a higher infection fatality rate due to limited hospital capacity. A lockdown, which we model as an income tax, reduces labor supply in order to reduce COVID-19 transmission. A lockdown can lower mortality by either containing the virus or by “flattening the curve,” that is slowing the virus’ spread such that demand for COVID-19 treatment does not exceed the health systems’ capacity. However, the reduction in labor supply and consequent consumption losses increase child mortality in low- and middle-income country settings.

We calibrate the model to 85 countries across all income groups to quantify the tradeoff between the expected number of COVID-19-related deaths averted by lockdowns and the number of lives lost to the resulting economic contractions. The COVID-19-related processes in the model are calibrated based on early data reported in the health literature, country-specific epidemiological projections ([Walker et al., 2020](#)), and patterns of social contacts in developing and developed countries. Implicitly, the analysis adopts the information set at the disposal of policymakers towards the start of the pandemic as countries initially formulated policy responses, before the emergence of possibly more infectious viral lineages ([Davies et al., 2021](#)).

Low-, middle-, and high-income countries differ along several relevant dimensions. First, economic contractions raise child mortality in poorer countries, but not in rich ones. We estimate that a percent decrease in per capita GDP can increase under-5 mortality by up to 0.15 deaths per 1,000 children in the poorest countries. Second, the demographic composition of poorer countries features a larger ratio of young children to old people. Since the survival of the former is put at risk by an economic downturn while the latter are most vulnerable to dying from COVID-19, a lockdown in lower-income countries leads to more recession-induced deaths per COVID-19 fatality averted, *ceteris paribus*. Third, a smaller share of social contacts are in the context of work or consumption in developing countries compared to developed ones. The preponderance of community-related transmission in low-income countries renders government-mandated lockdowns comparatively less effective at reducing the spread of infections. Finally, low health care capacity in poorer countries lowers the efficacy of a lockdown at “flattening the curve” as hospitals are quickly overwhelmed. The average number of hospital beds per capita in high-income countries is seven times higher than in low-income countries.²

To highlight the heterogeneity in outcomes, we subject each of the 85 countries in our sample to a uniform *reference* lockdown that lasts 7 weeks. We compare the economic and mortality outcomes in the reference lockdown to a scenario without any government intervention. The duration and the strength of the reference lockdown is chosen based on experiences in seven European countries in the start of the pandemic (Flaxman et al., 2020).³

Our main quantitative result is that there is substantial variation in health outcomes across countries following the reference lockdown. In our model, the lockdown led to an average of 1.76 child deaths for every COVID-19 fatality averted in low-income countries.

²The average number of hospital beds per 1,000 people was 0.8 and 5.7 in low- and high-income countries respectively in 2006, the last year for which the World Development Indicators data allow the comparison.

³We take the perspective of the initial months of the COVID-19 pandemic when governments were first confronted with designing pandemic responses in the absence of effective vaccines or therapeutics. We implement only non-pharmaceutical interventions because in the event of a new but similar pandemic, the same tradeoffs will be relevant as new vaccines and/or therapeutics would most likely not be immediately available. According to the Oxford Blavatnik COVID-19 Government Response Tracker, every single one of the 175 countries that it covers imposed at least some lockdown policy. Lockdown severity was remarkably similar across countries at different levels of development. On a scale of 0 to 100, the mean Oxford–Blavatnik lockdown stringency index was 79 in the low-income countries, and 78 in the high-income countries. (These averages are as of April 2020, the most globally synchronized phase of the lockdown. We use the World Bank classification of countries into income groups.)

The ratio falls to .59 and .06 in the case of lower-middle and upper-middle income countries, respectively. (By assumption, there is no mortality tradeoff in high-income countries.) As a result, lockdowns lower the total mortality by 6.2 percent in the richest countries, but *raise* total mortality by 2.6 percent in the poorest ones. The main country characteristics driving the heterogeneity in health outcomes are (i) the semi-elasticities of child mortality with respect to GDP and (ii) demography, as poorer countries are also younger countries.

Finally, we consider a utilitarian approach to setting lockdown policies, in which the social planner trades off averted deaths from COVID-19 averted against loss of life due to reduced GDP and the loss of consumption. The optimal lockdown varies across countries, as marginal costs and benefits are heterogeneous. Poor countries with younger populations generally impose shorter and milder lockdowns, as the governments internalize the impacts on child mortality. Thus, the optimal lockdown significantly reduces the share of the population infected in the rich countries but not in the poor countries. In the end, the child mortality impact is smaller as well: among the poorest countries, the optimal lockdown would lead to only 0.32 child deaths for every COVID-19 fatality averted.

Our paper complements the burgeoning body of work on the macroeconomic impact of the COVID-19 pandemic (see, among others, [Atkeson, 2020](#); [Alvarez et al., 2020](#); [Barrot et al., 2020](#); [Baqae and Farhi, 2020a,b](#); [Bonadio et al., 2020](#); [Glover et al., 2020](#); [Kaplan et al., 2020](#); [Krueger et al., 2020](#)). Most closely related are [Eichenbaum et al. \(2020\)](#), who develop an SIR-macro model, and [Acemoglu et al. \(2020\)](#), who model population heterogeneity by age. We customize these macro frameworks to developing countries. Our analysis shares the developing country focus with [Alon et al. \(2020\)](#), [Barnett-Howell and Mobarak \(2020\)](#), [Loayza \(2020\)](#), or [Ravallion \(2020b\)](#) who also point out differences between rich and poor countries in the benefits and costs of a lockdown and ultimately come to the same conclusion that the tradeoffs are different and country-specific. Our analysis highlights and more importantly quantifies a distinct mechanism, whereby a lockdown potentially increases child mortality in poorer countries.⁴ Other work that has surmised the potential toll for infant and child health as a consequence of the COVID19 pandemic includes [Robertson et al.](#)

⁴One underlying mechanism by which a lockdown increases child mortality is through deteriorating food security and was posited by [Ravallion \(2020a\)](#).

(2020), who use a health care seeking and supply model, and posit reductions in care seeking and available quality of care. In contrast, our approach uses the historical record of past contractions to calibrate the under-5 mortality semi-elasticity with respect to the economic shock.

The rest of the paper is structured as follows. Section 2 lays out the quantitative framework. In section 3, we discuss the data used to calibrate the model. The results are presented in section 4. Section 5 concludes. The Appendix contains additional details on theory and quantification.

2 Quantitative Framework

In this section, we build a macro-SIR model along the lines of Eichenbaum et al. (2020) with the added feature that households comprise several members in different age groups (Acemoglu et al., 2020). Our key innovations are (i) to model income shocks as a source of mortality not related to COVID-19; and (ii) to calibrate the model to 85 countries with different underlying characteristics.

2.1 Economic Environment

We consider a discrete and infinite time horizon model, $t = 0, 1, \dots, \infty$, and a continuum of households indexed by $j \in [0, 1]$. The measure of households is normalized to 1 in the initial period. Households are formed by individuals differentiated by age group $m \in \{1, 2, 3\}$ to which they belong. Type $m = 1$ individuals are children ages 0-14, type $m = 2$ are working prime-age adults ages 15-59 and $m = 3$ household members are the elderly aged 60 and over. Denote by ℓ^m the mass of individuals of age group m so that $\sum_{m=1}^3 \ell^m = 1$. We omit country indices in the model exposition to streamline notation, but in the quantitative analysis the model is implemented on a large sample of countries with country-specific parameter values.

Household j evaluates its lifetime utility according to:

$$U_j = \sum_{t=0}^{\infty} \beta^t u(\bar{c}_{jt}, n_{jt}), \quad (1)$$

where $\beta \in (0, 1)$ is the discount factor and $u(\cdot)$ is the instantaneous utility function, which takes the form

$$u(\bar{c}_{jt}, n_{jt}) = \bar{c}_{jt} - \frac{\theta}{2} n_{jt}^2, \quad (2)$$

where \bar{c}_{jt} is aggregate consumption of household j in period t and n_{jt} is the amount of labor it supplies, while θ drives the disutility of supplying labor.

Household consumption \bar{c}_{jt} aggregates individual consumption $c_{jt}(m)$ of all members of the household:

$$\bar{c}_{jt} = \left[\sum_{m=1}^3 \ell^m (c_{jt}(m))^{\frac{\sigma-1}{\sigma}} \right]^{\frac{\sigma}{\sigma-1}}, \quad (3)$$

where σ is the elasticity of substitution.

COVID-19 SIR states COVID-19 related health status is relevant for both disease transmission and economic behavior. Each individual can be in one of four states: susceptible (S), infected (I), recovered (R), or deceased (D). One feature of our model is that death can be due to either COVID-19 or another cause. We thus index each household state with integer $k \in \{1, \dots, 64\}$, which uniquely identifies a triplet $\{\zeta(1), \zeta(2), \zeta(3)\}$, where $\zeta(m) \in \{S, I, R, D\}$ indicates the health status of individual m . Appendix Table A.1 reports the list of possible household states.⁵

Labor supply, lockdown policy, and government budget In our model, only the prime-age adult ($m = 2$) household members supply labor. They are paid a wage w_t , which the government can tax at rate μ_t . As in Eichenbaum et al. (2020), the tax rate μ_t will be the instrument by which the policy maker implements a lockdown.⁶ Tax revenues are then

⁵Note that to reduce the dimensionality of the state space, we make the assumption that within households, all members in the same age group are in the same state. We thus do not allow two children (or adults or elderly) to be in two different states. While this assumption may be unrealistic at the household level, this simplification does not affect analysis at the aggregate level.

⁶We interpret “lockdown” policies broadly to include other forms of containment policies, such as encouraging social distancing, restricting public events, school and border closures, and so on.

remitted to households in a lump-sum manner. The budget constraint of household j is:

$$c_{jt} = \sum_{m=1}^3 \ell^m c_{jt}(m) \leq \begin{cases} (1 - \mu_t) w_t n_{jt} + \Gamma_{jt}, & \mathbf{S}_{jt}(2) = 1 \text{ or } \mathbf{R}_{jt}(2) = 1 \\ (1 - \mu_t) w_t \phi n_{jt} + \Gamma_{jt}, & \mathbf{I}_{jt}(2) = 1 \\ \Gamma_{jt}, & \mathbf{D}_{jt}(2) = 1 \end{cases} \quad (4)$$

where c_{jt} is total household consumption. Household income on the right-hand-side of (4) consists of after-tax labor income and government transfer Γ_{jt} . This budget constraint applies to the households with a susceptible ($\mathbf{S}_{jt}(2) = 1$) or recovered ($\mathbf{R}_{jt}(2) = 1$) working adult. If the working adult is infected ($\mathbf{I}_{jt}(2) = 1$), the effective labor supply falls to $\phi n_{jt} \leq n_{jt}$. Lastly, after the death of the working adult ($\mathbf{D}_{jt}(2) = 1$), household j lives off government transfers.

The amount Γ_{jt} transferred to households is determined by the government's budget constraint, i.e.

$$\int_{j=0}^1 \Gamma_{jt} dj = \mu_t w_t \left(\int_{j=0}^1 \mathbf{S}_{jt}(2) n_{jt} dj + \int_{j=0}^1 \mathbf{R}_{jt}(2) n_{jt} dj + \phi \int_{j=0}^1 \mathbf{I}_{jt}(2) n_{jt} dj \right) + \bar{\Gamma}_t, \quad (5)$$

where $\bar{\Gamma}_t$ is some exogenous development assistance revenue.

Firms There is a continuum of competitive firms of unit measure that produce consumption goods C_t using aggregate labor input N_t :

$$C_t = AN_t. \quad (6)$$

Firms choose total labor input to maximize their profit, Π_t :

$$\Pi_t = AN_t - w_t N_t, \quad (7)$$

In equilibrium, good and labor market clearing conditions are thus

$$C_t = \int_{j=0}^1 c_{jt} dj,$$

$$N_t = \int_{j=0}^1 \mathbf{S}_{jt}(2)n_{jt} dj + \int_{j=0}^1 \mathbf{R}_{jt}(2)n_{jt} dj + \phi \int_{j=0}^1 \mathbf{I}_{jt}(2)n_{jt} dj.$$

2.2 Mortality and Disease Transmission

We incorporate a modified SIR model to our macroeconomic framework. In our model there are three types of mortality risks: (i) economic distress risk, (ii) a COVID-19-related risk, and (iii) an exogenous baseline risk.

Economic distress and baseline mortalities An individual in age group m faces increased mortality during an economic downturn. A downturn is a downward deviation from baseline consumption, where baseline consumption is the consumption level that would be achieved in time $t = 0$ in the absence of a labor tax, i.e. $\mu = 0$, and is denoted \tilde{c}_j . Thus, for household j , a contraction takes place when faced with a positive labor tax or in the case of death of a prime-age working adult. In addition, in each period t an individual draws an exogenous age-group specific baseline death shock with probability $\bar{\pi}_n(m)$.

The economic distress mortality cum baseline mortality probability is:

$$\pi_{njt}(m) = \begin{cases} \bar{\pi}_n(m) & c_{jt} \geq \tilde{c}_j \\ \bar{\pi}_n(m) + \nu(m) \left(1 - \frac{c_{jt}}{\tilde{c}_j}\right) & c_{jt} < \tilde{c}_j \end{cases}, \quad (8)$$

where $\nu(m)$ is the elasticity of economic distress-related mortality with respect to the fluctuations in consumption. Importantly, in our quantification $\nu(m)$ will vary by country income level: it will be positive in poorer countries and decreasing in the income level. In rich countries economic distress-related mortality elasticity $\nu(m)$ will be 0. In the quantification, $\nu(m)$ will be positive only for children ($m = 1$).

COVID-related mortality The infection status of an individual of age group m in household j at time t is denoted $\mathbf{I}_{jt}(m) \in \{0, 1\}$. Thus, the mass of infected individuals at time t

is given by

$$I_t = \int_{j=0}^1 \sum_{m=1}^3 \ell^m \mathbf{I}_{jt}(m) dj.$$

Conditional on contracting COVID-19, The probability of death from the infection takes the following form:

$$\pi_{dt}(m) = \pi_d^m + \kappa^m(I_t), \quad (9)$$

where π_d^m is a baseline infection fatality rate and $\kappa^m(\cdot)$ measures how mortality also depends on the total infection rate. The function $\kappa^m(\cdot)$ reflects the possibility that a larger epidemic will lead to higher mortality due to saturation of health services such as ICU beds, oxygen ventilators, etc. (Yang et al., 2020).

In each period, the probability $\pi_{djt}(m)$ that an individual j will die combines both COVID-19 and non-COVID mortality risks. We make the assumption that the economic distress and COVID-19 mortality probabilities are orthogonal to each other in the cross-section of households. In that case, the death probability of a person of type m in household j becomes:

$$\pi_{djt}(m) = \begin{cases} 1 - [1 - \pi_{njt}(m)] [1 - \pi_{dt}(m)] & \text{if } \mathbf{I}_{jt}(m) = 1 \\ \pi_{njt}(m) & \text{if } \mathbf{I}_{jt}(m) = 0 \end{cases}. \quad (10)$$

Lockdown policies and COVID-19 disease dynamics Adapting the model of Eichenbaum et al. (2020), we assume that the transmission of the infection occurs through four channels: (i) the labor channel, whereby the infection spreads through workplace interactions, (ii) the consumption channel, which comprises contacts occurring while shopping for goods, (iii) the community channel, which represents all other interaction of individuals across households, and (iv) the within-household channel, to account for higher exposure of individuals who share residence with an infected individual.

A lockdown policy, therefore, will affect transmission likelihood through these same channels. As a tax on labor income, a lockdown reduces individual labor supply and consequently

lowers household consumption. Both lead to a decrease infection rates. We further allow a lockdown policy to mitigate community-related transmission with a semi-elasticity of ξ by imposing restrictions on social gatherings that affect community spread. We do not directly model decisions related to such gatherings and therefore account for the impact of lockdowns on community spread this way.

The probability that a susceptible individual m in household j will get infected in period t is given by:

$$\pi_{I_{jt}}(m) = \begin{cases} \pi_{I1}c_{jt}C_{It} + \pi_{I2}n_{jt}N_{It} + \pi_{I3}I_t(1 - \xi\mu_t) + \pi_{I4}\mathbf{I}_{jt}, & m = 2 \\ \pi_{I3}I_t(1 - \xi\mu_t) + \pi_{I4}\mathbf{I}_{jt}, & m = 1, 3 \end{cases}. \quad (11)$$

The first line of the equation above describes the infection probability of the working adult. The first three elements reflect transmission through consumption, labor supply, and the community, respectively, while the last part captures within-household transmission. Consumption and labor supply transmissions are a function of the aggregate consumption and labor supply of the infected individuals in period t C_{It} and N_{It} , which equal:

$$C_{It} = \int_{j=0}^1 \sum_{m=1}^3 \ell^m c_{jt}(m) \mathbf{I}_{jt}(m) dj,$$

$$N_{It} = \phi \int_{j=0}^1 n_{jt} \mathbf{I}_{jt}(2) dj.$$

Community transmission, on the other hand, is a function of the total number of infected people, I_t , as defined above. Finally, for within-household transmission, \mathbf{I}_{jt} , equals to one if any member of the household j is infected, and zero otherwise. The second line of equation (11) applies to the children and the elderly, who will only be infected through the community or within-household transmission channels, since they do not work and are assumed not to get exposed through consumption-related activities.

The total number of newly infected individuals T_t is thus given by:

$$T_t = \int_{j=0}^1 \sum_{m=1}^3 \ell^m \pi_{I_{jt}}(m) \mathbf{S}_{jt}(m) dj, \quad (12)$$

where $\mathbf{S}_{jt}(m)$ is an indicator function that takes the value of 1 when member m of household j is susceptible, and 0 otherwise. The number of susceptible individuals, S_t , evolves according to

$$S_{t+1} = S_t - T_t. \quad (13)$$

In period t , all infected individuals will receive the “recovery” shock. With probability $\pi_{rt}(m)$, the member recovers, with probability $\pi_{dt}(m)$ s/he dies, and with probability $\pi_{it}(m)$ s/he stays infected. Note that $\pi_{rt}(m) + \pi_{dt}(m) + \pi_{it}(m) = 1$. The number of infected individuals thus evolves according to:

$$I_{t+1} = \int_{j=0}^1 \sum_{m=1}^3 \ell^m \mathbf{I}_j(m) \pi_{it}(m) dj + T_t, \quad (14)$$

which consists of previously infected people who remain so for one additional period and newly infected individuals.

2.3 Household Optimization

We now turn to household optimization, subject to the aggregate states of the economy as summarized by $\Theta_t = \{C_{It}, N_{It}, I_t\}$ and government policy μ_t . We first note that all the households in state k face the same maximization problem and make the same decision. As a result, we use the subscript k instead of j to indicate the variables for all households in state k .

Consumption and labor supply Before solving the dynamic problem, we first solve the within-period problem by backward induction so to express household instantaneous utility as a function of their labor supply only and then optimize accordingly.

As we abstract away from saving and risk-sharing across households, the solution to the consumption problem is static and is characterized by a binding budget constraint $c_{kt} = (1 - \mu_t) \mathbf{1}_{kt}(2) w_t n_{kt} + \Gamma_{kt}$, where $\mathbf{1}_{kt}(m)$ is an indicator function that takes the value of one if member m of household in state k is alive. In light of this observation, we can re-write the

probability of death specified in equation (10), $\pi_{dkt}(m)$, as a function of labor supply:

$$\pi_{dkt}(n_{kt}; m) = \begin{cases} \bar{\pi}_n(m) + \nu(m) \left[1 - \frac{(1-\mu_t)\mathbf{1}_{kt}(2)w_t\phi n_{kt} + \Gamma_{kt}}{\bar{c}_k} \right] + \pi_d^m + \kappa^m(I_t) & \text{if } \mathbf{I}_{kt}(m) = 1 \\ \bar{\pi}_n(m) + \nu(m) \left[1 - \frac{(1-\mu_t)\mathbf{1}_{kt}(2)w_t n_{kt} + \Gamma_{kt}}{\bar{c}_k} \right] & \text{if } \mathbf{I}_{kt}(m) = 0 \end{cases}. \quad (15)$$

Similarly, the probability of the adult contracting COVID-19 can also be re-expressed as a function of labor supply:

$$\pi_{Ikt}(n_{kt}; 2) = \pi_{I1} [(1 - \mu_t) w_t n_{kt} + \Gamma_{kt}] C_{It} + \pi_{I2} n_{kt} N_{It} + \pi_{I3} I_t + \pi_{I4} \mathbf{I}_k. \quad (16)$$

Lastly, the standard property of CES aggregation implies that we can also re-write the flow utility function as a function of labor supply:

$$u(c_{kt}, n_{kt}) = \left[\sum_{m=1}^3 \ell^m [c_{kt}(m)]^{\frac{\sigma-1}{\sigma}} \right]^{\frac{\sigma}{\sigma-1}} - \frac{\theta}{2} n_{kt}^2,$$

in which the individual level consumption is equal to

$$c_{kt}(n_{kt}; m) = \frac{\mathbf{1}_{kt}(m)}{\sum_{m'=1}^3 \ell^{m'} \mathbf{1}_{kt}(m')} [(1 - \mu_t) w_t n_{kt} + \Gamma_{kt}].$$

Combining the two and simplifying:

$$u(n_{kt}) = [(1 - \mu_t) w_t n_{kt} + \Gamma_{kt}] \left[\sum_{m=1}^3 \ell^m \mathbf{1}_{kt}(m) \right]^{\frac{1}{\sigma-1}} - \frac{\theta}{2} n_{kt}^2. \quad (17)$$

Dynamic optimization With the solution of the consumption problem in hand, we can turn to the dynamic problem of a household in state k . The Bellman equation for household in state k can be written

$$U_{kt}(\Theta_t) = \max_n u(n) + \beta \sum_{k'=1}^K \rho_{kk'}(n|\Theta_t) U_{k',t+1}(\Theta_{t+1}), \quad (18)$$

subject to the transition probabilities from state k to k' , $\rho_{kk'}(\cdot)$, that depend on the aggregate state of the economy Θ_t .

The first-order condition determines optimal labor supply n_{kt} :

$$u'(n_{kt}) + \beta \sum_{k'=1}^K \frac{\partial}{\partial n} \rho_{kk'}(n_{kt}|\Theta_t) U_{k',t+1}(\Theta_{t+1}) = 0, \quad (19)$$

which takes the form

$$u'(n_{kt}) + \Lambda_{kt} = 0,$$

with $\Lambda_{kt} = \beta \sum_{k'=1}^K \frac{\partial}{\partial n} \rho_{kk'}(n_{kt}|\Theta_t) U_{k',t+1}(\Theta_{t+1})$. We can also write the optimal labor decision as

$$n_{kt} = \frac{[\sum_{m=1}^3 \ell^m \mathbf{1}_{kt}(m)]^{\frac{1}{\sigma-1}} (1 - \mu_t) w_t + \Lambda_{kt}}{\theta}. \quad (20)$$

First, note that in the absence of capital accumulation, households' labor decisions will only affect a subset of the transition probabilities, $\rho_{kk'}$. Labor supply only affects the probability of infection of the workers (the young adults) and the non-COVID mortality rate of children (since we assume that excess mortality from an economic contraction only affects children). All the other mortality rates, infection rates, and recovery rates follow a process that is not influenced by the decision of atomistic agents but depend on aggregate state Θ_t . We thus state the following result (proof available in the Appendix):

Lemma 1: First-order conditions The first-order condition for the household in state k , period t is:

$$\frac{\partial u}{\partial n_{kt}} + \lambda_{\pi_I}^k [\pi_{I1}(1 - \mu_t)w_t C_{It} + \pi_{I2}N_{It}] - \lambda_{\pi_d}^k \nu(1) \frac{(1 - \mu_t)w_t}{\tilde{c}_k} = 0, \quad (21)$$

where $\lambda_{\pi_I}^k$ is the Lagrangian multiplier on the infection probability, $\pi_{Ikt}(2)$:

$$\lambda_{\pi_I}^k = \beta (1 - \pi_{nkt}(2)) \left\{ \sum_{k'(2)=I} \rho_{kk'}(1|\Theta_t)\rho_{kk'}(3|\Theta_t)U_{k'} - \sum_{k'(2)=S} \rho_{kk'}(1|\Theta_t)\rho_{kk'}(3|\Theta_t)U_{k'} \right\}, \quad (22)$$

and $\lambda_{\pi_d}^k$ is the Lagrangian multiplier for the non-COVID child mortality rate, $\pi_{dkt}(1)$:

$$\lambda_{\pi_d}^k = \beta \left\{ \sum_{k'(1)=D} \rho_{kk'}(2|\Theta_t)\rho_{kk'}(3|\Theta_t)U_{k'} - \sum_{k'(2)\neq D} \rho_{kk'}(2|\Theta_t)\rho_{kk'}(3|\Theta_t)U_{k'} \right\}. \quad (23)$$

■

For households without a susceptible prime-age adult, $\lambda_{\pi_I}^k = 0$ as the terms inside the curly bracket in equation (22) are equal to zero. Similarly, $\lambda_{\pi_d}^k = 0$ for households without a child as the terms inside the curly bracket in equation (23) are equal to zero.

The first-order condition captures the tradeoff between a static optimization (i.e. a tradeoff between consumption and leisure) and the health risk of increased exposure through consumption and labor. Lemma 1 describes the heterogeneity in households' responses to the pandemic, as a function of their demographic composition and the health status of their members. On the one hand, labor decisions have no dynamic implications when no prime-age adult is susceptible. On the other hand, incentives to increase (resp. decrease) labor supply depend on whether there are children (resp. susceptible elderly people) in the household.

Equilibrium An equilibrium of the economy in period t is defined by a vector of labor supply decisions $\{n_{kt}\}_{k \in \{1, \dots, K\}}$ such that n_{kt} is a solution to (18) for some given Θ_{t+1} , and Θ_{t+1} is in turn determined by transition probabilities (11) and (10). To solve for the equilibrium, therefore, we propose the following algorithm:

Solution algorithm Take the policy vector, μ_t , as given. Start with a guess of n_{kt} for all $k = 1, \dots, K$ and $t = 1, \dots, T$.

1. Given the initial conditions, simulate the model forward from $t = 1$ to T to generate

S_t, I_t, R_t and D_t , as well as all the transition probabilities.

2. Infer U_{kt} for every k in the following steps. The details are discussed in the appendix.
 - (a) Compute the post-pandemic steady state values of U_k for all k .
 - (b) Compute backwards from the post-pandemic state T to 1 for all the U_{kt} .
3. Infer $\lambda_{\pi_d^k, t}$ and $\lambda_{\pi_I^k, t}$ from the first-order conditions of $\pi_{dkt}(1)$ and $\pi_{Ikt}(2)$, conditional on U_{kt} .
4. Infer n_{kt} from the first-order conditions of n_{kt} . Iterate on n_{kt} until convergence.

3 Data and Calibration

The strength and duration of a lockdown are critical aspects of our quantitative analysis. Our *reference* lockdown policy attempts to mimic what had been observed in the first weeks of the pandemic. It is henceforth defined by three parameters: its starting time, length, and strength. To calibrate these parameters alongside transmission rate parameters, we proceed in two steps. In the first step, we calibrate the transmission parameters, $\pi_{I1}, \dots, \pi_{I4}$, to match the relative importance of the different transmission modes and the overall predicted infection rate in an unmitigated spread scenario. In the second step, we calibrate the effect of lockdown severity on community transmission, ξ , alongside the strength of lockdown, $\bar{\mu}$, to jointly match the decline in GDP and the reproduction number, R_0 , as estimated by [Flaxman et al. \(2020\)](#) for European countries early in the pandemic.

3.1 Infection and Mortality Parameter Calibration

The within-household transmission parameter, π_{I4} , is taken from a meta-analysis of household transmission estimates from different settings. [Lei et al. \(2020\)](#) estimate the secondary infection rate in the household to be 0.27. To discipline the three other transmission parameters, we jointly match three moments.

The first moment is the proportion of the population that would get infected in each country in the absence of any mitigating policy. We use projections reported by [Walker et](#)

al. (2020), that use country- and age-specific contact patterns to simulate health impacts of COVID-19 in 202 countries. They develop an SIR model incorporating the age distribution of each country. Employing a basic reproduction number (R_0) of 3.0, they project that about 90 percent of the population would ultimately either recover from infection or die in an unmitigated epidemic scenario in lower- and middle-income countries. The unmitigated epidemiological model in Walker et al. (2020) assumes no behavioral response to the pandemic. For consistency, we assume that households continue to supply labor and consume at the same levels as in the pre-pandemic steady state in this stage of the calibration exercise. This assumption is relaxed in the following steps of the calibration.

The other two moments used for the calibration of the transmission parameters are the shares of infections occurring through labor and consumption. As most of the world's population lives in urban areas, we chose to use data reported by Johnstone-Robertson et al. (2011) on locations of contacts in a South African township community.⁷ The authors define close contacts as those involving physical contact or a two-way conversation with three or more words. They find the 6.2 percent of such contacts take place in workplaces while 3.5 percent of such contacts take place in shops or local bars and therefore can be thought of as related to consumption. 8.9 percent of such contacts take place during transport and could theoretically be linked to either labor or consumption. We assume that half of the transport is related to labor and half to consumption. This implies that 10.6 percent of contacts are related to work and 8 percent to consumption. For high-income countries, we use the rates employed by Eichenbaum et al. (2020) for the US. Based on analysis of the Bureau of Labor and Statistics 2018 Time Use Survey data and contact patterns reported in Ferguson et al. (2006) and Lee et al. (2010), they conclude that 16 percent of transmissions are related to consumption and 17 percent of transmissions are related to work.

⁷We reviewed the public health literature on social contacts in low- and middle-income countries and found no nationally representative study. Most of the studies focus on age-specific contacts and only a handful of studies categorized interpersonal contacts in a manner that permitted direct mapping into consumption and labor components.

3.2 Reference Lockdown and Community Transmission Parameter

Conditional on the transmission parameters calibrated previously, we calibrate the reference lockdown policy, and the parameter determining the relationship between lockdown strength and reduction in community transmission, ξ .

A country starts to impose the reference lockdown when the infected population reaches 2.6%. This rate is based on the prevalence at the time of the first lockdown in the Italian municipality of Vo, the site of the first COVID-19-related death detected in Italy (Lavezzo et al., 2020). In our calibration, the countries start to impose the reference lockdown policy between week 9 and 13, with an average start date at week 11.

The length of the reference lockdown policy is based on Flaxman et al. (2020) that estimates the impacts of non-pharmaceutical interventions in 11 European countries during the first months of the pandemic.⁸ We drop the four countries that only imposed mild or no lockdown policies (Denmark, Norway, Sweden, and Switzerland) and work with the remaining seven countries.⁹ We compute the lockdown length for each country based on the difference between the reported lockdown date and the end of the sample period in Flaxman et al. (2020). The lockdown policies range between 43 to 54 days, with an average of 7 weeks, which we use as the length of the reference lockdown. The strength of the lockdown was inferred from the GDP decline in the first two quarters of the year 2020. As explained later in this section, we calibrate $\theta = 1$, which implies that a lockdown policy of $\bar{\mu}$ reduces aggregate labor supply and GDP by $\bar{\mu}$. Therefore, an x -day lockdown reduces the two-quarter GDP by $x\bar{\mu}/180$, from which one can infer $\bar{\mu}$, conditional on the length of the lockdown calibrated above and the observed decline in GDP. For example, the inferred $\bar{\mu}$ in Germany with a 6.68 percent decline in GDP and a 43-day lockdown is $\bar{\mu} = 0.0668 * 180/43 = 0.2796$. We repeat the calculation for all seven countries and find that the strength of the lockdown policy to

⁸Out of the five non-pharmaceutical interventions studied in Flaxman et al. (2020), we focus on “lockdowns” to quantify the reference lockdown. Note that the “lockdown” in our model should be interpreted broadly to include the other four forms of intervention policies in Flaxman et al. (2020), such as social distancing, self-isolation, school closure, and restricting public events.

⁹The four countries with mild or no lockdown policies lead to corner solutions in the calibration of ξ , as explained below. The remaining 7 countries are Austria, Belgium, Britain, France, Germany, Italy, and Spain.

be between 28% and 46%. The average across the seven countries is 38%, which we use as $\bar{\mu}$ for the reference policy.

Given the country-specific $\bar{\mu}$ and lockdown length in these 7 countries, we can then compute ξ , the elasticity of community transmission with respect to lockdown, for each of these countries. To do this, we simulate the model and target the post-lockdown R_0 of 0.66 as reported in [Flaxman et al. \(2020\)](#) for the sample countries. The corresponding R_0 at period t in our model is computed as $\frac{T_{t-1}/I_{t-1}}{\pi_{rt} + \pi_{dt}}$, where π_{rt} and π_{dt} are the population-weighted average recovery and mortality rates in period t . We take the R_0 at the period after the lockdown policy ends, as the counter-part of the post-lockdown reproduction number in [Flaxman et al. \(2020\)](#). The resulting ξ ranges between 1.9 to 3.5 among the 7 countries with an interior solution, and we take the average of 2.32 to apply to all the 86 countries in the full sample.¹⁰

3.3 Mortality Rates

We look to two distinct literatures to calibrate our mortality parameters.

COVID-19 mortality [Walker et al. \(2020\)](#) projects hospitalization and mortality rates per age group that are in turn based on findings from China reported by [Verity et al. \(2020\)](#).¹¹ Conditional on infection, the average projected hospitalization and mortality rates in low- and middle-income countries are listed in [Table 1](#). In the calibration of the model, we use country-specific rates as countries have different age distributions within the broader age groups defined in our model.

¹⁰A corner solution in this step occurs for the four countries that we have dropped (Denmark, Sweden, Switzerland, and Norway). If the country imposes a mild lockdown, the implied $\bar{\mu}$ for this country will be low, which makes it impossible to reach the target R_0 even with $\xi = \infty$.

¹¹Infection fatality rates calculated with data from China might not be generalizable to other countries because of factors such as prevalence of comorbidities and quality of health services ([Ghisolfi et al., 2020](#); [Demombynes, 2020](#)). More recent meta-analyses found mortality rates in line with those reported by [Verity et al. \(2020\)](#) ([Levin et al., 2020](#); [Meyerowitz-Katz and Merone, 2020](#)). It is important to note, however, that these analyses overwhelmingly rely on studies from high-income countries.

Table 1: Mortality and Hospitalization Rates by Age

Age group	Hospitalization	Mortality
0-14	0.0009	0.00003
15-60	0.023	0.001
>60	0.130	0.034

Note: Average hospitalization and mortality rate by age group in low- and middle-income countries.

Source: [Walker et al. \(2020\)](#).

For severe cases of COVID-19 infection, hospitalization offers treatments such as oxygen therapy for patients with respiratory failure. Therefore, the case fatality rate (CFR) for a COVID-19 infection warranting hospital care but cannot access it is believed to be elevated. For example, [Yang et al. \(2020\)](#) find that the CFR by the middle of February 2020 within the city of Wuhan, China, the presumed outbreak location of origin for COVID-19, was substantially higher (5.25 percent) than in regions outside Wuhan but within the same province (1.41 percent) and in regions outside the province (0.15 percent). While the CFRs within and outside Wuhan should vary for several reasons, including availability of testing, a key factor was the initial demand for hospital beds exceeded the supply. For these reasons, we assume that the COVID-related mortality is elevated by a factor of 3 for those patients who are in need of hospitalization but cannot receive it.

We denote by $\pi_b(m)$ the probability an individual of group m requires hospitalization, conditional on being infected. The share of individuals in need of hospital beds at time t , B_t , is given by

$$B_t = \pi_b(1)I_t(1) + \pi_b(2)I_t(2) + \pi_b(3)I_t(3).$$

We assume that hospital bed allocation is random among those in need. Denoting by h to be the number of hospital beds, the probability that an infected individual dies at period t is given by

$$\pi_{idt}(m) = \begin{cases} \pi_{nt}(m) + \pi_d(m) & \text{if } B_t \leq h \\ \pi_{nt}(m) + (1 - \pi_b(m)) \pi_d(m) + \pi_b(m) \left(\frac{k}{B_t} \pi_d(m) + \frac{B_t - k}{B_t} 3\pi_d(m) \right) & \text{if } B_t > h \end{cases}$$

As in [Atkeson \(2020\)](#) and [Eichenbaum et al. \(2020\)](#), we assume that it takes an average of 18 days from infection to either recover or die. To obtain weekly mortality probabilities, we multiply the rates obtained from [Walker et al. \(2020\)](#) by 7/18.

The number of hospital beds in each country is obtained from the World Bank’s World Development Indicators. It should be noted that the most recent data available are from 2015 and that data for many countries is from even earlier years. In low- and middle-income countries, the average number of hospital beds per 1,000 people is 2.4.

Non-COVID-19 mortality Baseline mortality rates, $\bar{\pi}_{n1}$, $\bar{\pi}_{n2}$ and $\bar{\pi}_{n3}$ are computed from country-specific life table data obtained from the Global Health Observatory Data Repository of the World Health organization.¹²

In terms of elevated mortality due to shortfalls in aggregate income, several papers have estimated the relation between economic shocks and infant or young child mortality ([Baird et al., 2011](#); [Bhalotra, 2010](#); [Cruces et al., 2012](#); [Friedman and Schady, 2013](#); [Maruthappu et al., 2017](#)). For low and middle-income countries, the population groups most vulnerable to declines in aggregate income are young children and, perhaps, the elderly ([Cutler et al., 2002](#)). We focus on mortality impacts among children under-5 as this population group has been the most extensively studied. We estimate the effect of short-term aggregate income shocks on mortality following the methodology of [Baird et al. \(2011\)](#). We use data on GDP per capita from the World Development Indicators. The values are adjusted for purchasing power parity, corresponding to 2011 US dollars. Data on infant and child mortality are taken from retrospective birth histories as reported in the Demographic and Health Surveys (DHS) conducted in 83 low- and middle-income countries between 1985 and 2017. The combined sample is of 5.2 million births in low- and middle-income countries. We run regressions of the following form:

$$D_{ict} = \alpha_c + \beta \log \text{GDP}_{ct} + f_c(t) + \epsilon_{ict},$$

where D_{ict} is a binary indicator that takes the value 1 if child i in country c died in year t , $\log \text{GDP}$ is the natural logarithm of per capita GDP, $f_c(t)$ is a country-specific flexible time trend, and ϵ_{ict} is the error term. Standard errors are clustered at the country level.

¹²who.int/gho/data

We run the regression separately for countries of different income levels, as classified by the World Bank 2020 income groups. The main result is that a 1 percent decrease in per capita GDP is associated with a 0.15 increase in under-5 mortality per 1,000 children in low-income countries. The semi-elasticity is 0.1 and 0.03 for lower and upper middle-income countries, respectively. We assume that under-5 mortality is not impacted by income shocks in high-income countries. Unlike the results from low- and middle-income countries, studies analyzing data from the United States find mortality to be pro-cyclical (Ruhm, 2000; Dehejia and Lleras-Muney, 2004).

To map the estimated semi-elasticities into our calibration, we define s_{0-5} to be the share of children under five years old in the group of children of ages 0 to 15. The semi-elasticity of child mortality with consumption is given by

$$\nu_i(1) = s_{0-5}\beta_i, \quad i = \text{LIC, LMIC, UMIC},$$

where β_i represents the regression coefficients for low-, lower middle- and upper middle-income countries. $\nu(1)$ equals zero in high income countries. In addition, we also assume that mortality rates of the two older age groups are not responsive to income shocks.

It is possible that non-COVID child mortality will increase during the pandemic due to reduced coverage of essential health services (Robertson et al., 2020). If there is a disruption to supply of health services or if households avoid health facilities due to perceived risk of infection, our reduced-form estimation will not account for such pandemic-specific mechanisms. It is important to note, however, that these mechanisms will likely be at play regardless of the lockdown policy imposed by the government.

3.4 Demographic and Economic Parameters

Country-specific age distributions are obtained from the 2020 World Population Prospects.¹³ The age distribution is used to compute s_{0-5} , which is then used to rescale the semi-elasticity of under-5 mortality to the age group 0 - 15 using the formula above. In addition, we use the age distribution of the three age groups to compute the masses of the different age groups

¹³population.un.org/wpp

within the household (ℓ^1, ℓ^2, ℓ^3) in each country.

The weekly discount factor equals to $\beta = 0.96^{1/52}$ to reflect an annual risk-free rate of 4 percent. We assume that at $t = 0$, $\varepsilon = 0.1$ percent of population is infected. We set $\phi = 0.8$ so that an infected working adult is only 80 percent effective in supplying labor. This is equivalent to assume that 80 percent of the infected population is either asymptomatic or experiences a mild case.¹⁴ We set θ to 1 so that the steady state labor supply in the pre-pandemic world is normalized to 1 in all countries.

The parameter σ governs the elasticity of substitution between household members. We set it to 3, so that the loss of a non-productive household member – the children or the elderly – with mass ℓ^m reduces the instantaneous utility, $u(\cdot)$, by a proportion ℓ^m in steady state. Appendix B.3 provides the details of the derivation.

The values of $\bar{\Gamma}_t$ are calibrated based on the Atlas of Social Protection Indicators of Resilience and Equity (ASPIRE) data set. In the dataset, 1.55 percent of GDP was spent on social assistance programs on average. We assume that $\bar{\Gamma}_t$ is constant across the entire simulation, and calibrate it to be 1.55 percent of GDP in every country.

Lastly, we use the GDP in current US dollars from the World Bank’s World Development Indicators when computing the dollar amount of international aid required for each country.

Table 2 summarizes all the parameters of the model and indicates the data sources used to calibrate them.

4 Results

To quantitatively illustrate how the same policy might differently impact mortality outcomes in different countries, we compare two scenarios. The first scenario traces economic and disease-related behavior without any government intervention. The second scenario involves the reference lockdown as described above, where a labor tax of 38 percent is imposed for a seven-week period once the rate of infection prevalence reaches 2.6 percent. While the reference lockdown is determined to mimic policies adopted during the early months of the

¹⁴This corresponds to media reports on the results of an unpublished sero-prevalence study conducted in New York in April 2020 ([nytimes.com/2020/04/23/nyregion/coronavirus-antibodies-test-ny.html](https://www.nytimes.com/2020/04/23/nyregion/coronavirus-antibodies-test-ny.html)). [Li et al. \(2020\)](#) and [Stringhini et al. \(2020\)](#) report even higher rates of asymptomatic cases in China and Switzerland.

Table 2: Parameters

Name	Value	Source/Target	Note
π_{I1}	country-specific	share of transmission due to consumption-related activities	consumption-related activity transmission
π_{I2}	country-specific	share of infection due to work-related activities	work-related transmission
π_{I3}	country-specific	proportion of infected population	community-based infection
π_{I4}	0.27	Lei et al. (2020)	within-household infection
ξ	2.32	post-lockdown R_0 in	impact of lockdown on
-	country-specific	Flaxman et al. (2020), 7-country sample	community transmission
-	7	population infection rate of 2.6% lockdown length from	start date of the reference lockdown length of the reference lockdown
$\bar{\mu}$	38%	Flaxman et al. (2020), 7-country sample GDP decline in 2020Q1-Q2 in the 7 countries from Flaxman et al. (2020)	strength of the reference lockdown
semi-elasticity of child mortality w.r.t. income			
$\nu_j(1)$	0.15	Authors' estimation using DHS data	low-income countries
	0.10	Authors' estimation using DHS data	lower-middle income countries
	0.03	Authors' estimation using DHS data	upper-middle income countries
	0.00	Assumed based on literature	high-income countries
$\pi_d(m)$	country-specific	Walker et al. (2020)	COVID-19 mortality, type- m
$\pi_b(m)$	country-specific	Walker et al. (2020)	probability of hospitalization, type- m
k	country-specific	World Development Indicators	number of hospital beds per 1000 people
$\bar{\pi}_n(m)$	country-specific	WHO Global Health Repository	non-COVID mortality, type- m
$\ell(m)$	country-specific	World Population Prospects, 2020	mass of type- m
β	$0.96^{1/52}$	annual risk-free rate of 4 percent	weekly discount factor
ε	0.1%	Eichenbaum et al. (2020)	initial infected population
ϕ	0.8	Eichenbaum et al. (2020)	efficiency loss due to infection
θ	1.0	steady-state labor supply = 1	disutility from labor supply
σ	3.0	loss of type- m reduces $u(\cdot)$ by ℓ^m	elasticity of substitution between household members
$\bar{\Gamma}_t$	1.55% of GDP	ASPIRE dataset	external transfer payment

Note: this table lists the calibrated parameters discussed in the main text.

pandemic, it is not designed to capture all the complexities of mobility and social gathering restrictions imposed by various countries. Rather, the results below aim at highlighting the large heterogeneity in outcomes following the adoption of a uniform policy rule.

4.1 Lockdowns and Total Mortality

Figure 1 illustrates the reduction in adult COVID-related mortality as a result of the reference government-induced lockdown. The figure depicts adult excess mortality in the first year of the pandemic, were the reference lockdown to be implemented, relative to adult excess mortality in the no-action scenario. Excess mortality is calculated by subtracting the number of simulated adult deaths in the two scenarios by the number of adults simulated to die when the economy is not experiencing a COVID-19 outbreak.¹⁵ Overall, a single seven-week lockdown will reduce adult mortality from COVID-19 by less than 9 percent in all countries. The lockdown slows down the virus' spread but over a full-year horizon the effect on the total share of the population ever infected is small in many countries.

The figure also demonstrates that the policy efficacy of averting mortality through lockdown is correlated with countries' wealth. In low-income countries, an average of 3.5 percent of COVID-related deaths are averted, in comparison to an average of 6.2 percent in high-income countries. Several factors drive this pattern. First, wealthier countries' populations have a larger share of adults over 60, the group most at risk of dying from COVID-19. Second, because of greater hospital capacity in wealthier countries, a slowed pace of the virus' spread is more likely to translate into higher survival probabilities. Lastly, greater shares of transmission in high-income countries occur through labor and consumption-related contacts. Therefore, the reduced economic activity in these countries has a bigger impact on the virus transmission relative to countries where a larger share of transmissions occurs through community contacts.

Lockdowns and the mortality tradeoff Panel (a) of Figure 2 captures the inter-generational mortality tradeoff that is the focus of this paper. As in Figure 1, countries

¹⁵This calculation of excess mortality represents a minor underestimation of COVID-19 mortality. A share of adults who are simulated to die from COVID-19 might also receive a non-COVID mortality shock in the simulation of the no-COVID scenario. These deaths will not count towards the excess mortality calculation.

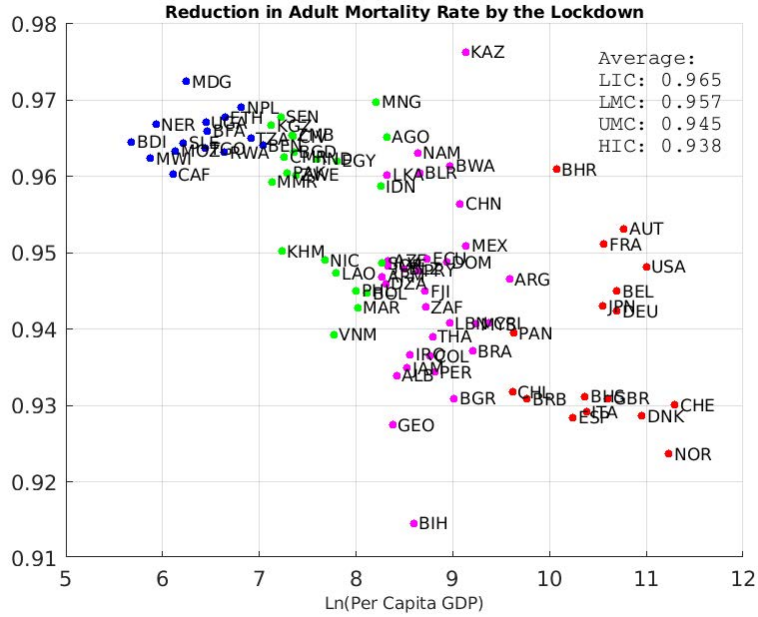
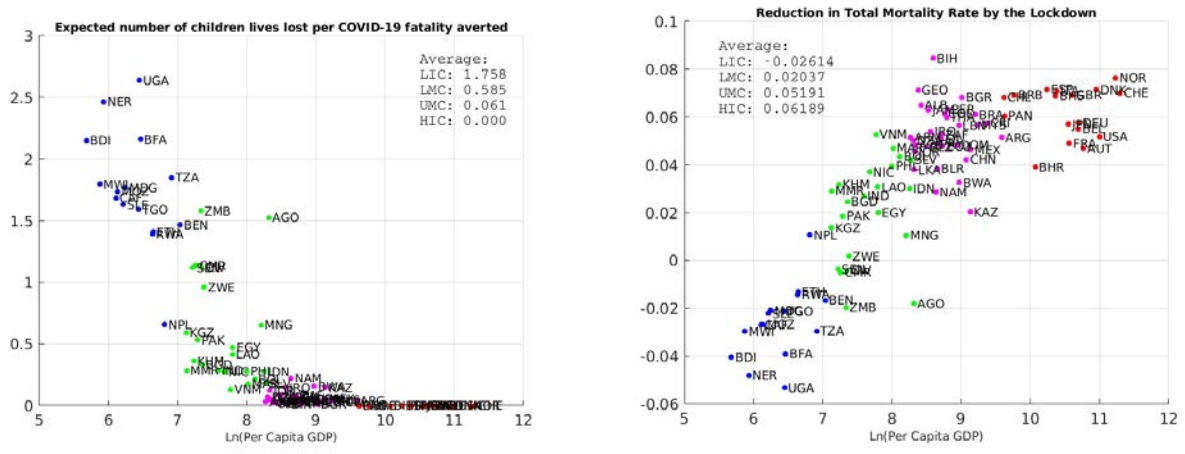


Figure 1: Impact of the reference lockdown on adult COVID-19 mortality

Note: This figure presents COVID-19 fatality averted against the logarithm of per capita GDP. The vertical axis presents the adult COVID-19 mortality during the first year of the pandemic in the reference lockdown scenario, as a fraction of COVID-19 mortality in the no-intervention scenario. Each dot represents a country and the color indicates the income group of the country: Low Income (blue), Lower-Middle-Income (green), Upper-Middle-Income (pink), and High-Income (red).

Source: World Development Indicators, Penn World Tables, and the authors' calculations.

are placed along the horizontal axis according to their log PPP-adjusted per capita income. The vertical axis represents the number of children's lives lost during the first year of the pandemic per every COVID-19 fatality averted by the reference lockdown. There is a pronounced negative relationship that arises from the different relationships between GDP contractions and infant mortality across income groups. By construction, no child life is lost due to COVID-19-related lockdowns in high-income countries, where we assume that GDP contractions have no impact on child mortality. High-income countries, therefore, lie on the horizontal axis. For lower-income countries, however, there can be a substantial loss of children's lives for each averted fatality from COVID-19. In 19 of the low- and lower-middle income countries in our sample, the reference lockdown policy leads to more children's lives lost than COVID-19 fatalities averted. In low-income countries, the reference lockdown causes an average of 1.76 child deaths per COVID-19 fatality averted. This rate is 0.59 in lower-middle income countries, and 0.06 in upper-middle income countries.



(a) Number of child deaths per COVID-19 fatality averted by the reference lockdown (b) Total reduction in mortality caused by the reference lockdown

Figure 2: Impact of the reference lockdown on total mortality

Note: Panel (a) presents the expected number of children lives lost per COVID-19 fatality averted against the logarithm of per capita GDP. Both the expected number of lives lost and the averted COVID-19 fatality are the differences between the reference lockdown policy and the no-intervention policy during the first year of the pandemic. Panel (b) presents the total reduction in mortality in the reference lockdown scenario, as a fraction of mortality in the no-intervention scenario. Each dot represents a country and the color indicates the income group of the country: Low Income (blue), Lower-Middle-Income (green), Upper-Middle-Income (pink), and High-Income (red).

Source: World Development Indicators, Penn World Tables, and the authors' calculations.

Lockdowns and total mortality Another informative statistic to compute is the effect of the reference lockdown on *total* mortality, which in effect puts equal weight on every life lost, irrespective of age. Panel (b) of Figure 2 plots the reduction in total excess mortality achieved by the lockdown, relative to excess mortality in the no-action policy against the logarithm of PPP-adjusted per capita GDP. The highest reductions in mortality are achieved in high-income countries where the lockdown has the highest impact in terms of preventing COVID-19-related deaths and does not impact child mortality. The implementation of the seven-week lockdown reduces the annual excess mortality by 6.2 percent in high-income countries. For low- and middle-income countries, the net reductions in total mortality are smaller in magnitude as the lockdown both has less impact on adult COVID mortality, and induces an increase in child mortality. In upper-middle and lower-middle income countries, mortality is reduced on average by 5.2 and 2 percent, respectively. In low-income countries, excess mortality will *increase* by 2.6 percent since the economic contraction leads to a higher

number of child deaths than the number of adult fatalities averted by the lockdown.

4.2 Understanding the Intergenerational Mortality Tradeoffs

The previous section illustrated the large variation in outcomes across countries due to the impact of the reference economic lockdown. In this section, we investigate the contributions of various country characteristics to the spread of the infection and subsequent mortality, both COVID-19-related and not.

4.2.1 Lockdown and the dynamics of the COVID-19 pandemic

To illustrate further what drives cross-country differences in outcomes, we present a more detailed analysis from four countries at different stages of economic development. We purposefully selected one country from each income group: Uganda (low income), Pakistan (lower-middle income), South Africa (upper-middle income), and the US (high income). These different income levels dictate how consumption shortfalls due to lockdown policies would affect child mortality. The selected countries also differ substantially along other dimensions that determine effectiveness of lockdown policies such as population age distribution and capacity of their health systems. Forty-six percent of the Ugandan population is under the age of 15 while only 3 percent are 60 years or older. In Pakistan and South Africa, respectively, 34 and 29 percent of the population are under 15 and 7 and 9 percent are 60 or older. The US has the oldest population out of the four countries, with only 18 percent under 15 and 23 percent 60 or older. Uganda and Pakistan have only 0.5 and 0.6 hospital beds per 1,000 people to contrast with rates in South Africa and the United States of 2.8 and 2.9, respectively.

Column (a) in Figure 3 displays the aggregate labor supply during the first year of the pandemic as a fraction of the no-pandemic steady-state labor supply. The blue line represents labor supply without any government intervention and the red line represents the reference lockdown scenario. Without any government action, there would be only small declines in labor supply during the weeks with the highest rates of active (current) infections (depicted in Panel (c) of the figure, solid blue line). The drop is entirely due to households

limiting their own labor supply to lower COVID-19 transmission risks to their own members. Relative to the other countries, the drop in labor supply is largest in the United States given its substantially larger share of older adults in the population. However, even in the United States the peak of the labor decline in the no-action scenario is less than five percent. This muted response reflects the sizeable externality associated with pandemics, i.e. households consider the tradeoff between their members' mortality risk and income loss but not the impact their exposure could have on the further spread of the virus in the population. Under the lockdown scenario, there will be a uniform reduction of 38 percent in labor supply during the weeks in which the labor tax will be in effect. Then there are subsequent additional small reductions in labor supply when active infections reach their highest rates. As in the no-action scenario, the subsequent reduction in labor supply is largest in the US but never exceeds five percent.

Columns (b) and (c) of Figure 3 illustrate how the lockdown policy affects virus transmission in the different countries. As can be seen in column (b), the seven-week lockdown will have only a negligible impact on the share of the population ever-infected by the end of the pandemic's first year. Instead, the lockdown slows the pace of transmission and displaces the peak infectivity period to later in the year. Overall, this policy more effectively slows the spread of the virus in wealthier countries. The infection rate peaks in Uganda and Pakistan before it does in South Africa and the US. The primary reason for that is that the share of working-age adults in the total population is larger in the wealthier countries and, hence, the reduced economic activity has a larger impact on transmission rates in South Africa and the US than it does in the other two countries.

Column (d) of Figure 3 depicts the cumulative all-cause child and adult mortality in the reference lockdown scenario, relative to the cumulative mortality in the no-lockdown scenario. In the three low- and middle-income countries, lockdown policies increase child mortality. This increase in child mortality is entirely due to the impact of the economic contraction induced by the lockdown policy. Given the high sensitivity of survival rates to income fluctuations in low-income countries, the largest increase in child mortality is caused by the lockdown in Uganda. In the United States, however, the lockdown policy reduces child mortality. Here this reduction is entirely associated with reduced COVID-related child

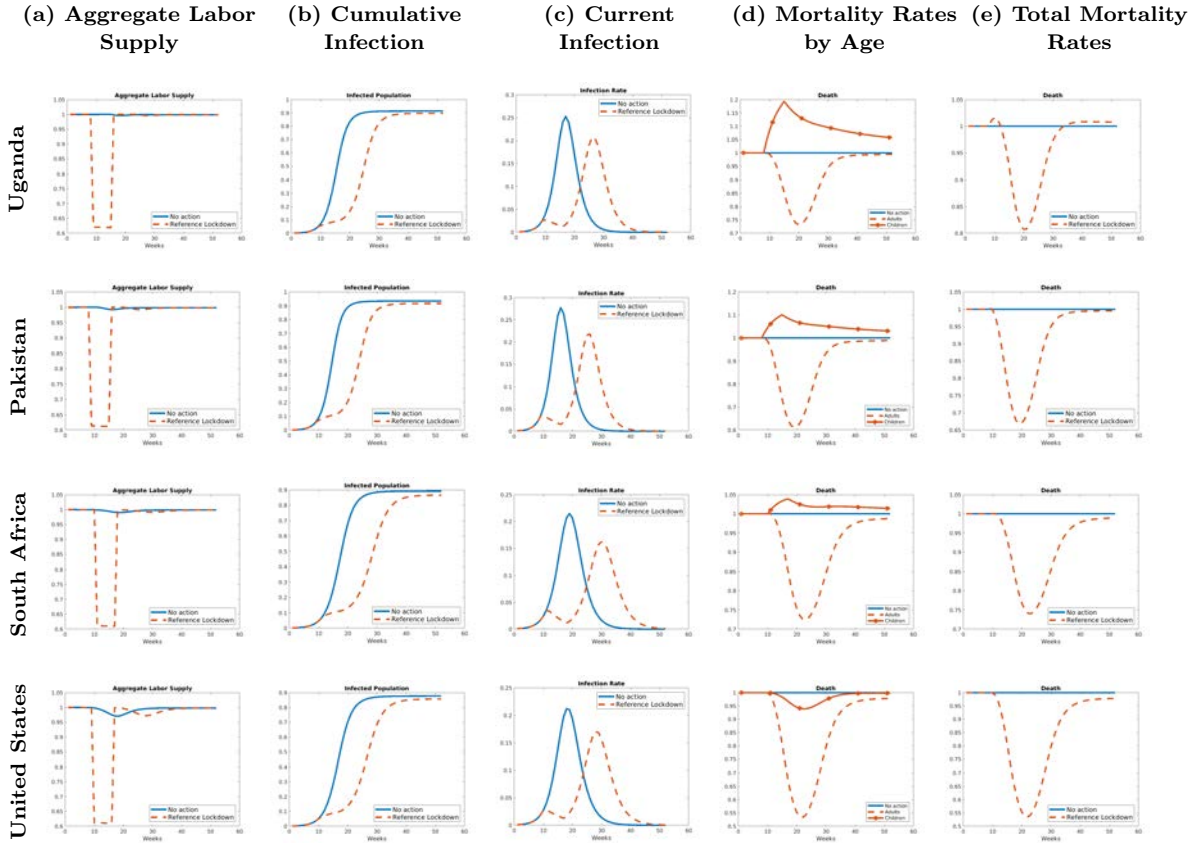


Figure 3: Selected Pandemic Indicators

Note: This figure presents several pandemic-related indicators for selected countries under a no action scenario (solid-blue line) and a reference lockdown scenario (dashed-red line). Column (a) presents the change in aggregate labor supply, relative to the pre-COVID-19 steady state. Column (b) presents the cumulative infection rate, where the total population is normalized to 1. Column (c) shows the contemporaneous infection rate in each week. Column (d) portrays the cumulative all-cause mortality rates (from both COVID-19 and non-COVID-19) separately for children and adults under the reference lockdown relative to the no intervention policy. Column (e) presents the total cumulative mortality rate of the reference lockdown policy relative to the no intervention policy.

Source: authors' calculation.

mortality, albeit from a low reference level.

With respect to adults, the reference lockdown temporarily reduces mortality in all countries. However, by the end of the first year of the epidemic, the single seven-week lockdown will have an average small effect on the cumulative adult mortality, as already shown in Figure 1. As highlighted above, the lockdown slows the spread of the virus by a number of weeks but has negligible impact on the cumulative rate of infections at the one-year horizon. Of the four countries, the 2 percent adult mortality reduction experienced in the US is the biggest due to several factors. First, the US has the highest share of adults over 60 who are

at greater risk of COVID mortality. Second, the lockdown is most effective in slowing down the virus spread in the US because of the differential modes of transmission. Third, because of higher hospital capacity, the slowdown in the virus spread causes a bigger improvement in survival rates.

Finally, column (e) of Figure 3 displays the total cumulative mortality rates in the lockdown scenario, expressed relative to the no-action mortality rate. In the poorest country of the four, Uganda, the total mortality in the lockdown scenario is *higher* than the no-action mortality rate by the end of the year. That is, the number of children who die from the decline in income is greater than the number of individuals' whose death is averted due to lockdown. In Pakistan, the excess child mortality is just slightly smaller than the modest adult mortality reduction achieved by the lockdown. In South Africa and the US, the lockdown achieved positive although small reductions in total deaths.

4.2.2 Decomposing the heterogeneity in policy impact

In this subsection we run counterfactual simulations to isolate various contributing mechanisms and gauge their influence on the overall cross-country variation in lockdown impacts.

Population age distribution In a first simulation, we impose the same age distribution for all countries, equal to the unweighted average age distribution across all 85 sample countries. Figure 4 is a scatterplot of the number of children's lives lost per COVID-19 fatality averted by the reference lockdown in this scenario (y-axis) against the baseline scenario. Relative to the results presented in Figure 2, the ratios are substantially lower when equalizing the age distribution in all countries. The ratio is below the 45-degree line and below 0.5 in value for all countries. This suggests that variation in the age distribution plays a crucial role in determining how the lockdowns affect overall mortality and the ratio of child deaths per COVID-19 fatality averted.

Country income In the second exercise, we keep the age structure of each country as is in the data but assign all countries the same per capita income and therefore the same semi-elasticity of child mortality with respect to income. The income level in each country

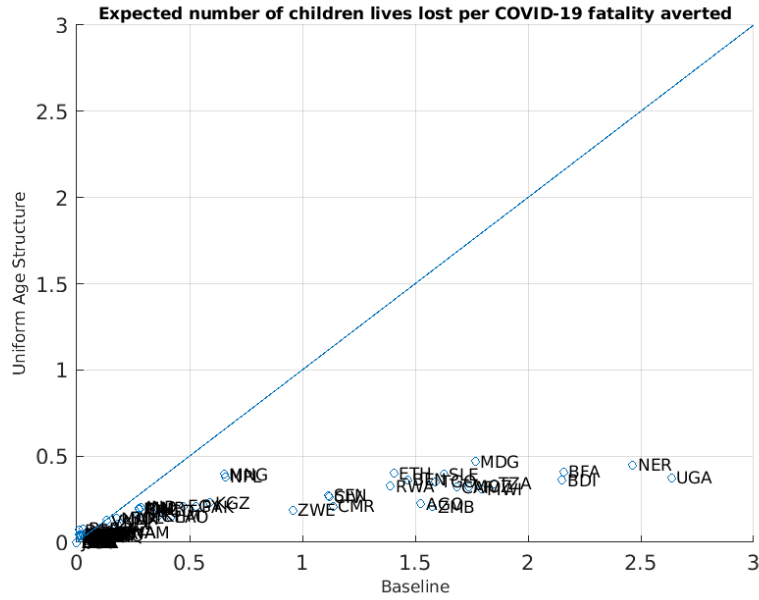


Figure 4: Decomposition: Constant age structure

Note: This figure presents the expected number of children lives lost per COVID-19 fatality averted in the baseline scenario against the counter-factual of constant age structure for all countries. Each dot represents a country. The solid blue line is the 45-degree line.

Source: authors' calculation.

in this example is the geometric average of per capita incomes in the sample, corresponding to a level within the upper-middle income designation. As can be seen in Figure 5, the variation in children's lives lost per COVID-19 fatality averted shrinks considerably in this counterfactual. This implies that the differences in income are even more important than age structure in determining the impact of lockdown policies on overall mortality, given the relationship between income shortfalls and child mortality in poorer countries.

Hospital capacity In the next simulation, we impose the US hospital capacity to all countries. As illustrated in Figure 6, the ratio of children lives lost per COVID-19 fatality averted increases for most low-income countries under such scenario. The reason is that with more extensive health systems, there are fewer COVID-19 fatalities under both the no-intervention and lockdown policies, leading to a smaller number of fatalities averted by the lockdown. It should be noted that in this simulation, health system capacity only affects COVID-related mortality. Improved health system capacity may also reduce also

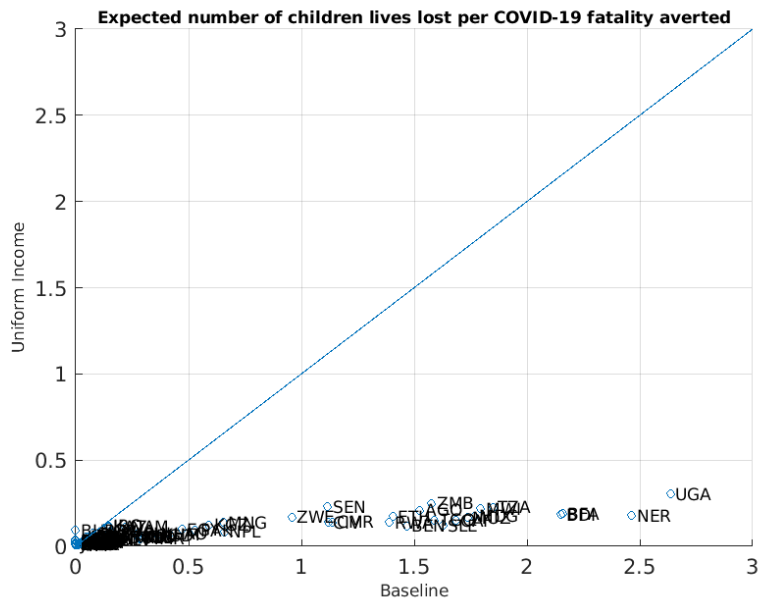


Figure 5: Decomposition: constant income

Note: This figure presents the expected number of children lives lost per COVID-19 fatality averted in the baseline scenario against the counter-factual. In the counter-factual, all the countries have the same income (within the upper middle-income range), and thus the same semi-elasticity of GDP fluctuations to child mortality. Each dot represents a country. The solid blue line is the 45-degree line. Source: authors' calculation.

non-COVID-related mortality and improve child survival resiliency to income shocks, but these channels are not incorporated in our model.

COVID-19 transmission shares by activity Finally, Figure 7 depicts a counterfactual in which transmission probabilities in all the countries are calibrated such that the share of transmission through each channel is similar to the U.S. As explained in the data section, the spread of COVID-19 in high-income countries is more reliant on work- and consumption-related activities, while more dependent on community transmission in developing countries. Therefore, the reference lockdown policy is more effective in slowing transmission in high-income countries, although the reduction in aggregate labor supply induced by the policy is identical in all countries. We see that the higher effectiveness of the reference lockdown leads to moderate declines in the ratio of child-lives lost per COVID-19 fatality averted. However, the change in transmission channel probabilities also affects the distribution of infections among the different age groups regardless of whether a lockdown is imposed. Because only

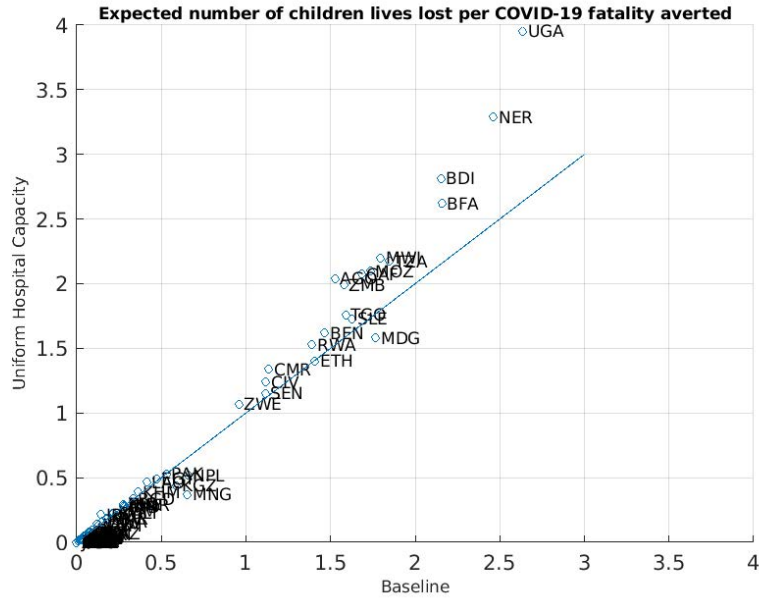


Figure 6: Decomposition: Constant hospital capacity

Note: This figure presents the expected number of children lives lost per COVID-19 fatality averted in the baseline scenario against the counter-factual. In the counter-factual, all the countries have the hospital capacity, measured as the number of hospital beds per thousand population. Each dot represents a country. The solid blue line is the 45-degree line.
 Source: authors' calculation.

working-age adults both supply labor and conduct consumption-related activities in our model, increasing the weight of these channels implies that a larger share of the initial infections would be among this group. Therefore, when the reference lockdown would be imposed (at a population prevalence of 2.6 percent), a smaller share of older adults would be infected at this point, and fewer deaths would be averted by the lockdown. This would push upwards the mortality ratio and explains why changing the transmission probabilities could increase the mortality ratio for some countries or only cause a moderate reduction in others.

Oaxaca-Blinder decomposition One way to assess the relative importance of the various mechanisms considered is to group all sample countries according to a binary distinction of low or high income, and then conduct an Oaxaca-Blinder decomposition including all factors explored individually above. This exercise (Table C.1 in the appendix) indicates three mechanisms absorb most of the cross-country variation in the relation between lockdown

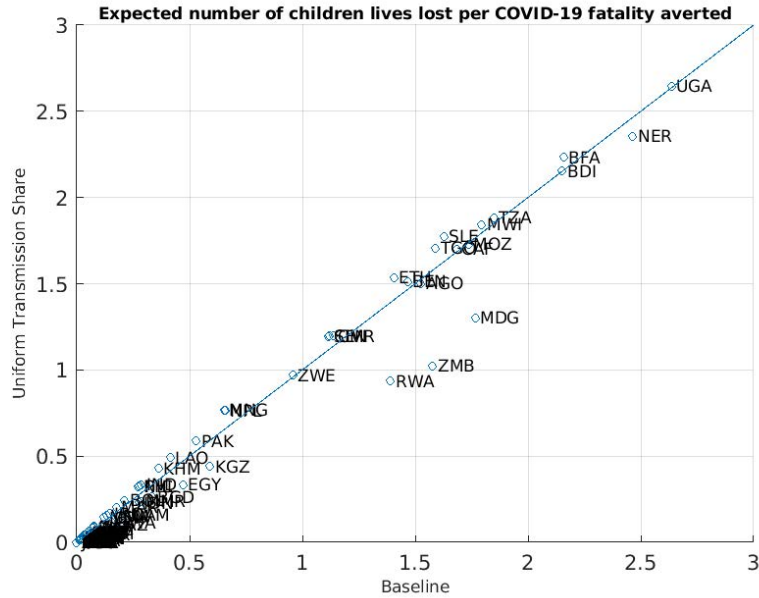


Figure 7: Decomposition: Constant transmission share

Note: this figure presents the expected number of children lives lost per COVID-19 fatality averted in the baseline scenario against the counter-factual. In the counter-factual, the π_{I1} , π_{I2} , and π_{I3} parameters in all the countries are calibrated to the same targets as the United States. Each dot represents a country. The solid blue line is the 45-degree line.
 Source: authors' calculation.

induced child mortality and averted COVID-19 deaths (these findings hold for the reference lockdown as well as the optimal lockdown discussed below). The most influential factor is the semi-elasticity of child mortality to economic contraction, which accounts for 80 percent of the explained variation across the two country groups. The share of the population under 15 years of age is also a significant factor, accounting for 29 percent of the explained variation. These two factors “explain” more than 100 percent of the variation across countries since other considered factors decrease the cross-country variation in the ratio of child deaths to averted COVID-19 deaths. The most significant factor that decreases this variation is the community transmission parameter. When community-based transmission constitutes a larger share of total COVID-19 disease transmission, any lockdown policy will be less effective in averting COVID-19 mortality, resulting in higher ratios of child deaths to averted COVID-19 deaths. These three considered factors are the only significant factors in the decomposition exercise. Other factors such as the share of the population 60 years or older, hospital capacity,

or the work and consumption related transmission parameters are not especially influential in explaining the observed variation in the tradeoff between child- and COVID-mortality.

4.3 Optimal Lockdown Policy

To conclude our discussion, we consider alternative lockdown policies that explicitly weigh COVID-19-related mortality against welfare more generally. We define an optimal lockdown policy as a labor tax sequence, $\{\mu_t\}$, that would lead to maximizing the present value of aggregate social welfare, i.e.

$$\max_{\{\mu_t\}} \int_{j=0}^1 U_j(\{\mu_t\}) dj.$$

As such, the optimality condition now captures the tradeoff between COVID-19 deaths and both increased infant mortality and the welfare loss due to reduced consumption. As the maximization problem does not yield a straightforward optimality condition, we use global maximization methods to search for the optimal lockdown policy.

Figure 8 depicts the ratio of child deaths per adult death averted by this lockdown policy. In comparison to the rates presented in Panel (a) of Figure 2 for the reference lockdown, the ratio of child to adult mortality under the optimal policy is substantially lower. The ratio for all countries is below 0.7 and Uganda is the only country with a ratio above 0.5. Thus, in contrast to the reference lockdown calibrated to mimic policies implemented by European governments in the first few months of the pandemic, the optimal lockdown never leads to a net mortality increase.

Figure 9 demonstrates how the optimal lockdown policies vary across the four selected countries considered above. Relative to the reference lockdown, the optimal lockdown policy would be milder in terms of labor contraction but start earlier and last longer in all countries. Column (a) of the figure also highlights that there are substantial differences in the length and severity of the optimal lockdowns in the four countries. There is a negative relation between a country's income level and the drop in labor supply induced by the optimal policy. Relative to the poorer countries, the lockdown in the US will be more severe as it has no impact on child mortality and is more effective in reducing transmission. In the US, lockdown measures

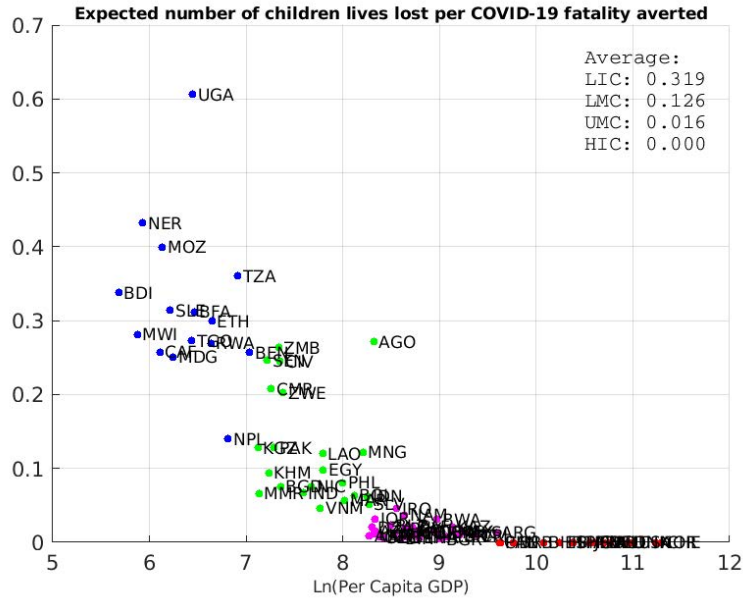


Figure 8: Number of child deaths per COVID-19 fatality averted by the optimal lockdown

Note: This figure presents the expected number of child lives lost per COVID-19 fatality averted against the logarithm of per capita GDP. Both the expected number of lives lost and the averted COVID-19 fatality are the differences between a lockdown policy and the no-intervention policy during the two years since the beginning of the pandemic. Each dot represents a country and the color indicates the income group of the country: Low Income (blue), Lower-Middle-Income (green), Upper-Middle-Income (pink), and High-Income (red).

Source: World Development Indicators, Penn World Tables, and the authors' calculations.

will be applied during the whole duration of the first year of the pandemic and the labor supply will decline by more than 25 percent when the current infection rate peaks. At the other extreme, Uganda will introduce lockdown measures only in the first half of the year and labor supply never drops below 90 percent of the pre-COVID rate.

As seen in column (b) of Figure 9, the optimal lockdown policy substantially reduces the share of the population that ever gets infected in South Africa and the US but not in Uganda and Pakistan. As a result, the optimal policy has a much larger impact on adult mortality in the wealthier countries, in comparison to the reference lockdown (column d). On the other hand, the optimal policy induces smaller increases in child mortality in the low- and middle-income countries.

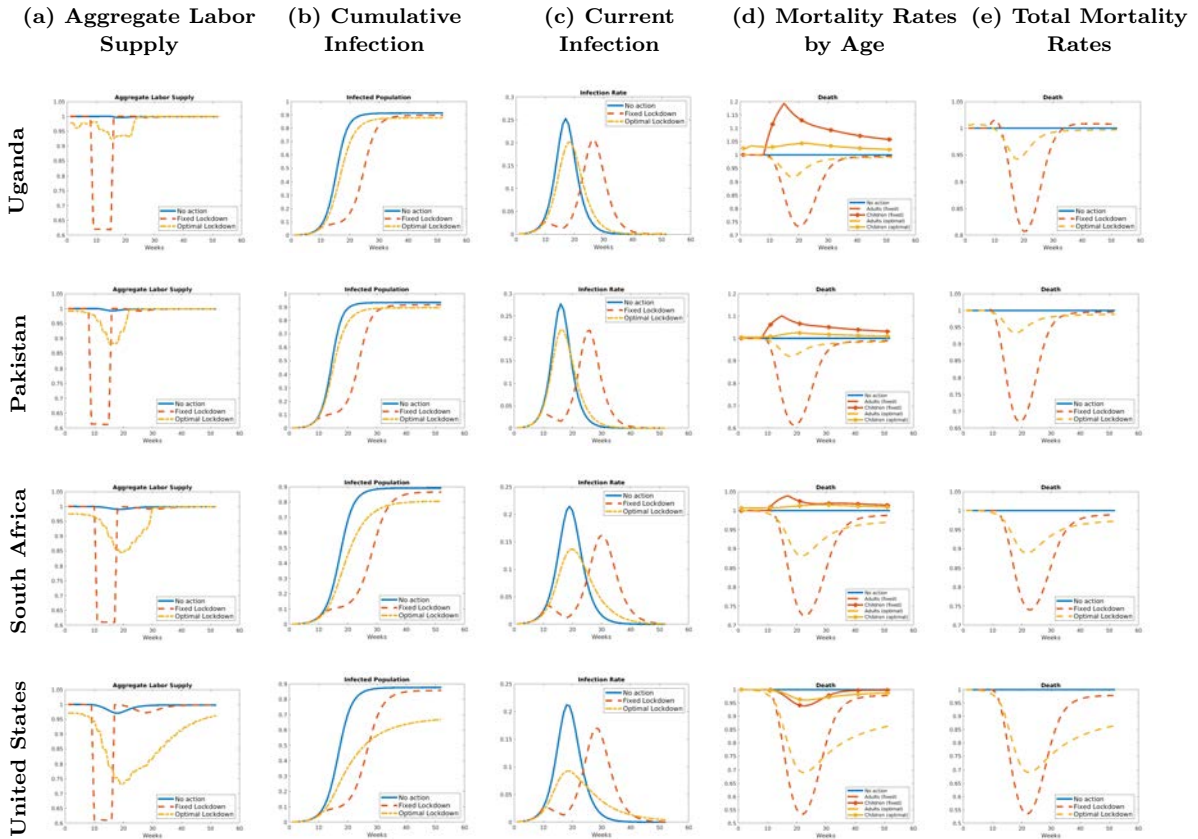


Figure 9: Selected Pandemic Indicators

Note: This figure presents several pandemic indicators for selected countries. Panels (a) present the cumulative infection rate, where the total population is normalized to 1. Panels (b) are the infection rate in each week. Panels (c) are the mortality rates of COVID-19 and non-COVID-19 under the optimal lockdown relative to the no intervention policy. Panels (d) present the total mortality rates of different lockdown policies relative to the no intervention policy. Panels (e) present the aggregate labor supply under different policies.

Source: authors' calculations.

5 Conclusion

At the start of the COVID-19 pandemic, countries around the world imposed lockdown measures similar in severity. Our analysis, however, suggests that optimal policies substantially differ, depending on the resiliency of child survival to income shocks, countries' demographic characteristics, and patterns of social contacts. The reason is that economic contractions in low- and middle-income countries have been tied to increased rates of child mortality. During the COVID-19 period, disease control responses have contributed to declines in national income for much of the world. This paper highlights and then quantifies this relatively

neglected consequence of disease control policies, thereby informing country-specific assessments of the costs and benefits of lockdowns as policies to fight a pandemic.

While our paper highlighted and quantified a tradeoff between human lives, namely children vs. adults, attenuating or mitigating it could be achieved with a second policy instrument such as targeted social assistance towards families with young children and pregnant women.

A more comprehensive evaluation of the tradeoffs underlying the use of disease control interventions would require considering a more exhaustive list of potential channels that go beyond the scope of this paper. For example, the pandemic and the policy responses to it are likely to affect coverage rates of essential health services which may result in additional detriments to population health than those considered here. On the health service supply-side, there are expected to be disruptions of supply chains and resource reallocation towards COVID-19-related activities. On the demand-side, users might avoid health facilities out of fear of infection or have their mobility constrained by lockdown policies. Such indirect health effects have been shown to substantially reduce coverage of maternal and child health services during the recent Ebola outbreak in West Africa ([Brolin Ribacke et al., 2016](#)).

Another, longer-run, cost of lockdowns may be detriments to human capital as a result of school closures and reduced household income. It is unclear if the lower investment in human capital over the pandemic period can or will be compensated by increased future investment. On the other hand, COVID-19 infections averted through control policies will also lower the incidence of any long-term health complications from COVID-19 infection survivors.

Finally, future work in the vein presented here would also need to rely on a better understanding (both qualitative and quantitative) of the policies chosen to address the current pandemic and the behavioral responses of private actors. While our model allows for some private response to infection likelihood, it may understate the extent of private protective behavior, at least in high-income countries ([Sheridan et al., 2020](#); [Atkeson et al., 2021](#)). In part due to the likely presence of behavioral responses, the extent to which government social distancing policies affect social contacts in all aspects of people's lives is an important yet under-investigated parameter, on which many quantitative assessments rely.

References

- Acemoglu, Daron, Victor Chernozhukov, Iván Werning, and Michael D Whinston**, “Optimal Targeted Lockdowns in a Multi-Group SIR Model,” December 2020. Forthcoming, *American Economic Review: Insights*.
- Alon, Titan M, Minki Kim, David Lagakos, and Mitchell VanVuren**, “How Should Policy Responses to the COVID-19 Pandemic Differ in the Developing World?,” May 2020. NBER Working Paper No. 27273.
- Alvarez, Fernando, David Argente, and Franceso Lippi**, “A Simple Planning Problem for COVID-19 Lockdown, Testing, and Tracing,” *American Economic Review: Insights*, 2020.
- Andreasen, Viggo, Cécile Viboud, and Lone Simonsen**, “Epidemiologic characterization of the 1918 influenza pandemic summer wave in Copenhagen: implications for pandemic control strategies,” *The Journal of infectious diseases*, 2008, 197 (2), 270–278.
- Atkeson, Andrew**, “What Will Be the Economic Impact of COVID-19 in the US? Rough Estimates of Disease Scenarios,” March 2020. NBER Working Paper 26867.
- Atkeson, Andrew G, Karen Kopecky, and Tao Zha**, “Behavior and the Transmission of COVID-19,” in “AEA Papers and Proceedings,” Vol. 111 2021, pp. 356–60.
- Baird, Sarah, Jed Friedman, and Norbert Schady**, “Aggregate income shocks and infant mortality in the developing world,” *Review of Economics and statistics*, 2011, 93 (3), 847–856.
- Baqae, David Rezza and Emmanuel Farhi**, “Nonlinear Production Networks with an Application to the Covid-19 Crisis,” April 2020. mimeo, UCLA and Harvard.
- and —, “Supply and Demand in Disaggregated Keynesian Economies with an Application to the Covid-19 Crisis,” April 2020. Mimeo, UCLA and Harvard.
- Barnett-Howell, Zachary and Mushfiq Mobarak**, “The Benefits and Costs of Social Distancing in Rich and Poor Countries,” April 2020. arXiv:2004.04867.
- Barrot, Jean-Noel, Basile Grassi, and Julien Sauvagnat**, “Sectoral Effects of Social Distancing,” April 2020. Mimeo, HEC-Paris and Bocconi.
- Bhalotra, Sonia**, “Fatal fluctuations? Cyclicalities in infant mortality in India,” *Journal of Development Economics*, 2010, 93 (1), 7–19.
- Bonadio, Barthélémy, Zhen Huo, Andrei A Levchenko, and Nitya Pandalai-Nayar**, “Global Supply Chains in the Pandemic,” May 2020. NBER Working Paper No. 27224.
- Cruces, Guillermo, Pablo Glüzmann, and Luis Felipe López Calva**, “Economic crises, maternal and infant mortality, low birth weight and enrollment rates: evidence from Argentina’s downturns,” *World Development*, 2012, 40 (2), 303–314.

- Cutler, David M, Felicia Knaul, Rafael Lozano, Oscar Méndez, and Beatriz Zurita**, “Financial crisis, health outcomes and ageing: Mexico in the 1980s and 1990s,” *Journal of Public Economics*, 2002, *84* (2), 279–303.
- Davies, Nicholas G, Sam Abbott, Rosanna C Barnard, Christopher I Jarvis, Adam J Kucharski, James D Munday, Carl AB Pearson, Timothy W Russell, Damien C Tully, Alex D Washburne et al.**, “Estimated transmissibility and impact of SARS-CoV-2 lineage B. 1.1. 7 in England,” *Science*, 2021, *372* (6538).
- Dehejia, Rajeev and Adriana Lleras-Muney**, “Booms, busts, and babies’ health,” *The Quarterly Journal of Economics*, 2004, *119* (3), 1091–1130.
- Demombynes, Gabriel**, “COVID-19 Age-Mortality Curves Are Flatter in Developing Countries,” 2020.
- Eichenbaum, Martin S, Sergio Rebelo, and Mathias Trabandt**, “The Macroeconomics of Epidemics,” Working Paper 26882, National Bureau of Economic Research March 2020.
- Ferguson, Neil M, Derek AT Cummings, Christophe Fraser, James C Cajka, Philip C Cooley, and Donald S Burke**, “Strategies for mitigating an influenza pandemic,” *Nature*, 2006, *442* (7101), 448–452.
- Flaxman, Seth, Swapnil Mishra, Axel Gandy, H Juliette T Unwin, Thomas A Mellan, Helen Coupland, Charles Whittaker, Harrison Zhu, Tresnia Berah, Jeffrey W Eaton et al.**, “Estimating the effects of non-pharmaceutical interventions on COVID-19 in Europe,” *Nature*, 2020, pp. 1–8.
- Friedman, Jed and Norbert Schady**, “How many infants likely died in Africa as a result of the 2008–2009 global financial crisis?,” *Health Economics*, 2013, *22* (5), 611–622.
- Garske, Tini, Anne Cori, Archchun Ariyaratnam, Isobel M Blake, Ilaria Dorigatti, Tim Eckmanns, Christophe Fraser, Wes Hinsley, Thibaut Jombart, Harriet L Mills et al.**, “Heterogeneities in the case fatality ratio in the West African Ebola outbreak 2013–2016,” *Philosophical Transactions of the Royal Society B: Biological Sciences*, 2017, *372* (1721), 20160308.
- Ghisolfi, Selene, Ingvild Almås, Justin C Sandefur, Tillman von Carnap, Jesse Heitner, and Tessa Bold**, “Predicted COVID-19 fatality rates based on age, sex, comorbidities and health system capacity,” *BMJ global health*, 2020, *5* (9), e003094.
- Glover, Andrew, Jonathan Heathcote, Dirk Krueger, and José-Víctor Ríos-Rull**, “Health versus Wealth: On the Distributional Effects of Controlling a Pandemic,” April 2020. CEPR Discussion Paper 14606.
- Hall, Robert E, Charles I Jones, and Peter J Klenow**, “Trading off consumption and covid-19 deaths,” Technical Report, National Bureau of Economic Research 2020.

- Jia, Na, Dan Feng, Li-Qun Fang, Jan Hendrik Richardus, Xiao-Na Han, Wu-Chun Cao, and Sake J De Vlas**, “Case fatality of SARS in mainland China and associated risk factors,” *Tropical Medicine & International Health*, 2009, *14*, 21–27.
- Johnstone-Robertson, Simon P, Daniella Mark, Carl Morrow, Keren Middekoop, Melika Chiswell, Lisa DH Aquino, Linda-Gail Bekker, and Robin Wood**, “Social mixing patterns within a South African township community: implications for respiratory disease transmission and control,” *American journal of epidemiology*, 2011, *174* (11), 1246–1255.
- Kaplan, Greg, Ben Moll, and Gianluca Violante**, “Pandemics According to HANK,” March 2020. mimeo.
- Karlberg, J, DSY Chong, and WYY Lai**, “Do men have a higher case fatality rate of severe acute respiratory syndrome than women do?,” *American journal of epidemiology*, 2004, *159* (3), 229–231.
- Kim, Young Eun and Norman V Loayza**, “Economic loss from COVID-19 fatalities across countries: a VSL approach,” *Applied Economics Letters*, 2021, pp. 1–7.
- Krueger, Dirk, Harald Uhlig, and Taojun Xie**, “Macroeconomic Dynamics and Reallocation in an Epidemic,” April 2020. CEPR Discussion Paper 14607.
- Lavezzo, Enrico, Elisa Franchin, Constanze Ciavarella, Gina Cuomo-Dannenburg, Luisa Barzon, Claudia Del Vecchio, Lucia Rossi, Riccardo Manganeli, Arianna Loregian, Nicolò Navarin et al.**, “Suppression of a SARS-CoV-2 outbreak in the Italian municipality of Vo’,” *Nature*, 2020, *584* (7821), 425–429.
- Lee, Bruce Y, Shawn T Brown, Philip C Cooley, Richard K Zimmerman, William D Wheaton, Shanta M Zimmer, John J Grefenstette, Tina-Marie Assi, Timothy J Furphy, Diane K Wagener et al.**, “A computer simulation of employee vaccination to mitigate an influenza epidemic,” *American journal of preventive medicine*, 2010, *38* (3), 247–257.
- Lei, Hao, Xiaolin Xu, Shenglan Xiao, Xifeng Wu, and Yuelong Shu**, “Household transmission of COVID-19—a systematic review and meta-analysis,” *Journal of Infection*, 2020, *81* (6), 979–997.
- Levin, Andrew T, William P Hanage, Nana Owusu-Boaitey, Kensington B Cochran, Seamus P Walsh, and Gideon Meyerowitz-Katz**, “Assessing the age specificity of infection fatality rates for COVID-19: systematic review, meta-analysis, and public policy implications,” *European journal of epidemiology*, 2020, pp. 1–16.
- Li, Ruiyun, Sen Pei, Bin Chen, Yimeng Song, Tao Zhang, Wan Yang, and Jeffrey Shaman**, “Substantial undocumented infection facilitates the rapid dissemination of novel coronavirus (SARS-CoV-2),” *Science*, 2020, *368* (6490), 489–493.
- Loayza, Norman**, “Macroeconomic Dynamics and Reallocation in an Epidemic,” May 2020. World Bank Research and Policy Brief no. 35.

- Maruthappu, Mahiben, Robert A Watson, Johnathan Watkins, Thomas Zeltner, Rosalind Raine, and Rifat Atun**, “Effects of economic downturns on child mortality: a global economic analysis, 1981–2010,” *BMJ global health*, 2017, 2 (2), e000157.
- Meyerowitz-Katz, Gideon and Lea Merone**, “A systematic review and meta-analysis of published research data on COVID-19 infection-fatality rates,” *International Journal of Infectious Diseases*, 2020.
- Olson, Donald R, Lone Simonsen, Paul J Edelson, and Stephen S Morse**, “Epidemiological evidence of an early wave of the 1918 influenza pandemic in New York City,” *Proceedings of the National Academy of Sciences*, 2005, 102 (31), 11059–11063.
- Pritchett, Lant and Lawrence H Summers**, “Wealthier is Healthier.,” *Journal of Human Resources*, 1996, 31 (4).
- Ravallion, Martin**, “Could Pandemic Lead to Famine?,” April 2020. Project Syndicate.
- , “Pandemic Policies in Poor Places,” April 2020. CGD Note.
- Ribacke, Kim J Brolin, Dell D Saulnier, Anneli Eriksson, and Johan von Schreeb**, “Effects of the West Africa Ebola virus disease on health-care utilization—a systematic review,” *Frontiers in public health*, 2016, 4, 222.
- Roberton, Timothy, Emily D Carter, Victoria B Chou, Angela R Stegmuller, Bianca D Jackson, Yvonne Tam, Talata Sawadogo-Lewis, and Neff Walker**, “Early estimates of the indirect effects of the COVID-19 pandemic on maternal and child mortality in low-income and middle-income countries: a modelling study,” *The Lancet Global Health*, 2020.
- Ruhm, Christopher J**, “Are recessions good for your health?,” *The Quarterly journal of economics*, 2000, 115 (2), 617–650.
- Sheridan, Adam, Asger Lau Andersen, Emil Toft Hansen, and Niels Johannesen**, “Social distancing laws cause only small losses of economic activity during the COVID-19 pandemic in Scandinavia,” *Proceedings of the National Academy of Sciences*, 2020, 117 (34), 20468–20473.
- Singer, Peter and Michael Plant**, “When Will the Pandemic Cure Be Worse Than the Disease?,” April 2020. Project Syndicate.
- Slovic, Paul and Ellen Peters**, “Risk perception and affect,” *Current directions in psychological science*, 2006, 15 (6), 322–325.
- Stringhini, Silvia, Ania Wisniak, Giovanni Piumatti, Andrew S Azman, Stephen A Lauer, Helene Baysson, David De Ridder, Dusan Petrovic, Stephanie Schrempft, Kailing Marcus et al.**, “Repeated seroprevalence of anti-SARS-CoV-2 IgG antibodies in a population-based sample from Geneva, Switzerland,” *medRxiv*, 2020.

- Verity, Robert, Lucy C Okell, Ilaria Dorigatti, Peter Winskill, Charles Whittaker, Natsuko Imai, Gina Cuomo-Dannenburg, Hayley Thompson, Patrick GT Walker, Han Fu et al.**, “Estimates of the severity of coronavirus disease 2019: a model-based analysis,” *The Lancet infectious diseases*, 2020.
- Viscusi, W Kip and Joseph E Aldy**, “The value of a statistical life: a critical review of market estimates throughout the world,” *Journal of risk and uncertainty*, 2003, 27 (1), 5–76.
- Walker, PGT, C Whittaker, O Watson et al.**, “The Global Impact of COVID-19 and Strategies for Mitigation and Suppression: WHO Collaborating Centre for Infectious Disease Modelling,” *MRC Centre for Global Infectious Disease Analysis, Abdul Latif Jameel Institute for Disease and Emergency Analytics, Imperial College London*, 2020.
- Yang, Shu, Peihua Cao, Peipei Du, Ziting Wu, Zian Zhuang, Lin Yang, Xuan Yu, Qi Zhou, Xixi Feng, Xiaohui Wang et al.**, “Early estimation of the case fatality rate of COVID-19 in mainland China: a data-driven analysis,” *Annals of translational medicine*, 2020, 8 (4).

A Additional Tables and Figures

Table A.1: Household states

k	States	Case	k	States	Case	k	States	Case
1	SSS	3	23	ISR	3	45	IDR	5
2	ISS	3	24	RSR	3	46	IRD	2
3	RSS	3	25	DSR	1	47	IRR	2
4	DSS	1	26	ISD	3	48	IDD	5
5	SIS	2	27	RSD	3	49	DIR	4
6	SRS	2	28	DSD	1	50	RID	2
7	SDS	5	29	IIS	2	51	RIR	2
8	SSI	3	30	RIS	2	52	DID	4
9	SSR	3	31	DIS	4	53	DRI	4
10	SSD	3	32	IRS	2	54	RDI	5
11	SII	2	33	RRS	2	55	RRI	2
12	SRI	2	34	DRS	4	56	DDI	5
13	SDI	5	35	IDS	5	57	RRR	2
14	SIR	2	36	RDS	5	58	DRR	4
15	SRR	2	37	DDS	5	59	RDR	5
16	SDR	5	38	III	2	60	RRD	2
17	SID	2	39	RII	2	61	RDD	5
18	SRD	2	40	DII	4	62	DRD	4
19	SDD	5	41	IRI	2	63	DDR	5
20	ISI	3	42	IDI	5	64	DDD	5
21	RSI	3	43	IIR	2			
22	DSI	1	44	IID	2			

Note: this table lists all the states that a household could be in. The three letters indicate the state of each of the three members of the household. “S” means that the member is susceptible, “I” for infected, “R” for recovered, and “D” for deceased. For example, for a household in state 53, “DRI”, children are deceased, adults recovered, and the elderly infected. “Case” refers to the cases used to prove Lemma 1, as detailed in Appendix B.1.

Table A.2: List of Countries

Low-income countries:			
Benin	Burkina Faso	Burundi	Central African Republic
Eritrea	Ethiopia	Madagascar	Malawi
Mozambique	Nepal	Niger	Rwanda
Sierra Leone	Tanzania	Togo	Uganda
Lower-middle income countries:			
Angola	Bangladesh	Bolivia	Cambodia
Cameroon	Cote d'Ivoire	Egypt, Arab Republic	El Salvador
India	Indonesia	Kyrgyz Republic	Lao PDR
Mongolia	Myanmar	Nicaragua	Pakistan
Philippines	Senegal	Vietnam	Zambia
Zimbabwe			
Upper-middle income countries:			
Albania	Algeria	Argentina	Armenia
Azerbaijan	Belarus	Belize	Bosnia and Herzegovina
Botswana	Brazil	Bulgaria	China
Colombia	Costa Rica	Dominican Republic	Ecuador
Fiji	Georgia	Iraq	Jamaica
Jordan	Kazakhstan	Lebanon	Malaysia
Mexico	Namibia	Paraguay	Peru
South Africa	Sri Lanka	Thailand	
High-income countries:			
Bahamas, The	Bahrain	Barbados	Chile
France	Italy	Japan	Panama
Spain	Sweden	United Kingdom	United States

Note: Countries included in the analysis by income group classification based on the World Bank grouping for fiscal year 2020.

B Model and Quantification

B.1 Proof of Lemma 1

First, note that we can divide the future states starting from any k into two categories: those k' that depend on n_{kt} and those that do not. We define the set of future states to which the transition probability that are independent from the household decision as \bar{K}_k :

$$\bar{K}_k = \{k' | \rho_{kk'}(n_{kt} | \Theta_t) = \rho_{kk'}(\Theta_t)\}.$$

All the infeasible states from k with $\rho_{kk'} = 0$ are also part of the set \bar{K}_k . With this insight we can re-write the household decision problem, highlighting that from the household's perspective, the transition probabilities into the states $k' \in \bar{K}_k$ will be taken as exogenously given:

$$U_k = u(n_{kt}) + \beta \left[\sum_{k' \in (K \setminus \bar{K}_k)} \rho_{kk'}(n_{kt} | \Theta_t) U_{k'} + \sum_{k' \in \bar{K}_k} \rho_{kk'}(\Theta_t) U_{k'} \right]. \quad (\text{B.1})$$

The household will internalize the dynamic effects of labor supply on 1) child mortality and 2) virus transmission through equations (15) and (16). In the rest of the section, we discuss all the possible combinations of these two dynamic effects.

Case 1, Infection Shock ($\pi_{Ikt}(2)$) Applicable In the first case, the household has a susceptible young adult but no children, and thus only the infection shock applies. We express the household problem as:

$$\begin{aligned} U_k &= u(n_{kt}) + \beta \pi_{Ikt}(2) (1 - \pi_{nkt}(2)) \sum_{k'(2)=I} \rho_{kk'}(1 | \Theta_t) \rho_{kk'}(3 | \Theta_t) U_{k'} \\ &\quad + \beta (1 - \pi_{Ikt}(2)) (1 - \pi_{nkt}(2)) \sum_{k'(2)=S} \rho_{kk'}(1 | \Theta_t) \rho_{kk'}(3 | \Theta_t) U_{k'} \\ &\quad + \sum_{k' \in \bar{K}_k} \rho_{kk'}(\Theta_t) U_{k'} \end{aligned} \quad (\text{B.2})$$

In the equation above, we separate the future states depending on the outcome of the young adult, $k'(2)$, which relies on the realization of $\pi_{Ikt}(2)$. We also use $\rho_{kk'}(m)$ denote the probability that the state of individual m will change from $k(m)$ to $k'(m)$ in the next period.¹⁶

$$\rho_{kk'}(n_{kt} | \Theta_t) = \prod_{m=1}^3 \rho_{kk'}(m | \Theta_t).$$

¹⁶The equation above implicitly relies on the assumption that the transition shocks are independent across family members. Note that the future states in which the young adult dies due to non-COVID reasons, $k'(2) = D$, are part of the set \bar{K}_k , and thus do not affect the policy function of the household.

Considering the transition probabilities, the Lagrangian of the household problem is:

$$\begin{aligned}
U_k &= u(n_{kt}) + \beta \pi_{Ikt}(2) (1 - \pi_{nkt}(2)) \sum_{k'(2)=I} \rho_{kk'}(1|\Theta_t) \rho_{kk'}(3|\Theta_t) U_{k'} \\
&+ \beta (1 - \pi_{Ikt}(2)) (1 - \pi_{nkt}(2)) \sum_{k'(2)=S} \rho_{kk'}(1|\Theta_t) \rho_{kk'}(3|\Theta_t) U_{k'} + \sum_{k' \in (\bar{K}_k)} \rho_{kk'}(\Theta_t) U_{k'} \\
&+ \lambda_{\pi_I}^k [\pi_{I1} [(1 - \mu_t) w_t n_{kt} + \Gamma_{kt}] C_{It} + \pi_{I2} n_{kt} N_{It} + \pi_{I3} I_t + \pi_{I4} \mathbf{I}_k - \pi_{Ikt}(2)],
\end{aligned}$$

where $\lambda_{\pi_I}^k$ is the multiplier associated with the transition probability. The FOC with respect to n_{kt} is

$$\frac{\partial u}{\partial n_{kt}} + \lambda_{\pi_I}^k [\pi_{I1} (1 - \mu_t) w_t C_{It} + \pi_{I2} N_{It}] = 0. \quad (\text{B.3})$$

Lastly, the FOC for $\pi_{Ikt}(2)$ is:

$$\beta (1 - \pi_{nkt}(2)) \left\{ \sum_{k'(2)=I} \rho_{kk'}(1|\Theta_t) \rho_{kk'}(3|\Theta_t) U_{k'} - \sum_{k'(2)=S} \rho_{kk'}(1|\Theta_t) \rho_{kk'}(3|\Theta_t) U_{k'} \right\} - \lambda_{\pi_I}^k = 0. \quad (\text{B.4})$$

Note that from the equation above, it is clear that $\lambda_{\pi_I}^k$ captures the drop in the future value if the young adult becomes infected in the next period. In other words, $\lambda_{\pi_I}^k$ is the value of staying uninfected during the pandemic.

Case 2, Child Mortality Shock ($\pi_{dkt}(1)$) Applicable In this case, the young working adult is either infected or recovered, and the children are alive. The Lagrangian equation is:¹⁷

$$\begin{aligned}
U_k &= u(n_{kt}) + \beta \pi_{dkt}(1) \sum_{k'(1)=D} \rho_{kk'}(2|\Theta_t) \rho_{kk'}(3|\Theta_t) U_{k'} \\
&+ \beta (1 - \pi_{dkt}(1)) \sum_{k'(1) \neq D} \rho_{kk'}(2|\Theta_t) \rho_{kk'}(3|\Theta_t) U_{k'} + \sum_{k' \in (\bar{K}_k)} \rho_{kk'}(\Theta_t) U_{k'} \\
&+ \lambda_{\pi_d}^k \left\{ \bar{\pi}_n(m) + \nu(m) \left[1 - \frac{(1 - \mu_t) w_t n_{kt} + \Gamma_{kt}}{\tilde{c}_k} \right] - \pi_{dkt}(1) \right\},
\end{aligned}$$

The FOC with respect to n_{kt} is:

$$\frac{\partial u}{\partial n_{kt}} - \lambda_{\pi_d}^k \nu(1) \frac{(1 - \mu_t) w_t}{\tilde{c}_k} = 0, \quad (\text{B.5})$$

and the FOC with respect to $\pi_{dkt}(1)$:

$$\beta \left\{ \sum_{k'(1)=D} \rho_{kk'}(2|\Theta_t) \rho_{kk'}(3|\Theta_t) U_{k'} - \sum_{k'(2) \neq D} \rho_{kk'}(2|\Theta_t) \rho_{kk'}(3|\Theta_t) U_{k'} \right\} - \lambda_{\pi_d}^k = 0. \quad (\text{B.6})$$

Similar to the previous case, the multiplier $\lambda_{\pi_d}^k$ captures the value of the children.

¹⁷Note that in the equation above, we have assumed that the children are not infected. Assuming infected children will only alter the level of $\pi_{dkt}(1)$ without affecting the first order conditions. The FOC also assumes that the young working adult is not infected. If the adult is infected, the FOC will be slightly modified to reflect the discount on productivity.

Case 3, Both Shocks Applicable When both the infection and the mortality shocks apply, the Lagrangian becomes:

$$\begin{aligned}
U_k = & u(n_{kt}) + \beta \pi_{dkt}(1) \pi_{Ikt}(2) [1 - \pi_{nkt}(2)] \sum_{k'(1)=D \cap k'(2)=I} \rho_{kk'}(3|\Theta_t) U_{k'} \\
& + \beta [1 - \pi_{dkt}(1)] \pi_{Ikt}(2) [1 - \pi_{nkt}(2)] \sum_{k'(1) \neq D \cap k'(2)=I} \rho_{kk'}(3|\Theta_t) U_{k'} \\
& + \beta \pi_{dkt}(1) [1 - \pi_{Ikt}(2)] [1 - \pi_{nkt}(2)] \sum_{k'(1)=D \cap k'(2)=S} \rho_{kk'}(3|\Theta_t) U_{k'} \\
& + \beta [1 - \pi_{dkt}(1)] [1 - \pi_{Ikt}(2)] [1 - \pi_{nkt}(2)] \sum_{k'(1) \neq D \cap k'(2)=S} \rho_{kk'}(3|\Theta_t) U_{k'} \\
& + \beta \pi_{dkt}(1) \pi_{nkt}(2) \sum_{k'(1)=D \cap k'(2)=D} \rho_{kk'}(3|\Theta_t) U_{k'} \\
& + \beta [1 - \pi_{dkt}(1)] \pi_{nkt}(2) \sum_{k'(1) \neq D \cap k'(2)=D} \rho_{kk'}(3|\Theta_t) U_{k'} + \sum_{k' \in (\bar{K}_k)} \rho_{kk'}(\Theta_t) U_{k'} \\
& + \lambda_{\pi_I}^k [\pi_{I1} [(1 - \mu_t) w_t n_{kt} + \Gamma_{kt}] C_{It} + \pi_{I2} n_{kt} N_{It} + \pi_{I3} I_t + \pi_{I4} \mathbf{I}_k - \pi_{Ikt}(2)] \\
& + \lambda_{\pi_d}^k \left\{ \bar{\pi}_n(m) + \nu(m) \left[1 - \frac{(1 - \mu_t) w_t n_{kt} + \Gamma_{kt}}{\tilde{c}_k} \right] - \pi_{dkt}(1) \right\}.
\end{aligned}$$

The FOC for labor supply is:

$$\frac{\partial u}{\partial n_{kt}} + \lambda_{\pi_I}^k [\pi_{I1} (1 - \mu_t) w_t C_{It} + \pi_{I2} N_{It}] - \lambda_{\pi_d}^k \nu(1) \frac{(1 - \mu_t) w_t}{\tilde{c}_k} = 0 \quad (\text{B.7})$$

and for $\pi_{Ikt}(2)$:

$$\beta (1 - \pi_{nkt}(2)) \left\{ \sum_{k'(2)=I} \rho_{kk'}(1|\Theta_t) \rho_{kk'}(3|\Theta_t) U_{k'} - \sum_{k'(2)=S} \rho_{kk'}(1|\Theta_t) \rho_{kk'}(3|\Theta_t) U_{k'} \right\} - \lambda_{\pi_I}^k = 0. \quad (\text{B.8})$$

Lastly, the FOC for $\pi_{dkt}(1)$:

$$\beta \left\{ \sum_{k'(1)=D} \rho_{kk'}(2|\Theta_t) \rho_{kk'}(3|\Theta_t) U_{k'} - \sum_{k'(2) \neq D} \rho_{kk'}(2|\Theta_t) \rho_{kk'}(3|\Theta_t) U_{k'} \right\} - \lambda_{\pi_d}^k = 0 \quad (\text{B.9})$$

Case 4, Neither Shocks Applicable In this case, the labor decision today does not affect the transition probability. As a result, the FOC of labor supply only takes the current utility into consideration:

$$\frac{\partial u}{\partial n_{kt}} = 0.$$

Case 5, No Young Adult In the four cases above, we have implicitly assumed that the young adult is alive. In the case of a deceased young adult, there is no optimization of problem for the household to solve. The remaining members of the household will consume the government transfer in every period.

B.2 Recursion

We use recursion to compute the post-pandemic steady state levels of U_k , as well as U_{kt} in the backward induction.

To infer the steady state U_k , the necessary condition is that $U_{k'}$ are known for all the $k' \neq k$ such that $\rho_{kk'} > 0$. In other words, we need to know the value of all the future states k' that state k can possibly transit into, except for k itself, in order to infer the value of state k . We start the recursion by assuming that no U_k is known. In the first iteration, the only state that can be inferred is the absorbing state, $k = 64$, in which all the agents are dead. In the second recursion, we can then infer all the states that are only one-step away from the absorbing state, $k = 61, 62, 63$. We repeat this process until all the U_k are known. The last state to infer is $k = 1$.

With the steady state U_k computed for all k , we then repeat this process for all $t = T, T-1, \dots, 1$ to compute all the U_{kt} . At $t = T$, we assume that the future states are steady state. For all $t < T$, the future states are simply $t + 1$.

B.3 Calibration of σ

From equation (20), it is straightforward to see that in the pre-pandemic steady state, $\Lambda_{kt} = 0$ and $\mu_t = 0$. Therefore the labor supply is reduced to:

$$n_k = \frac{[\sum_{m=1}^3 \ell^m \mathbf{1}_k(m)]^{\frac{1}{\sigma-1}} w_t}{\theta}. \quad (\text{B.10})$$

The instantaneous utility function in equation (17) simplifies to:

$$\begin{aligned} u(n_k) &= (w_t n_k) \left[\sum_{m=1}^3 \ell^m \mathbf{1}_k(m) \right]^{\frac{1}{\sigma-1}} - \frac{\theta}{2} n_k^2 \\ &= \left(\frac{[\sum_{m=1}^3 \ell^m \mathbf{1}_k(m)]^{\frac{1}{\sigma-1}} w_t^2}{\theta} \right) \left[\sum_{m=1}^3 \ell^m \mathbf{1}_k(m) \right]^{\frac{1}{\sigma-1}} - \frac{\theta}{2} \left(\frac{[\sum_{m=1}^3 \ell^m \mathbf{1}_k(m)]^{\frac{1}{\sigma-1}} w_t}{\theta} \right)^2 \\ &= \frac{[\sum_{m=1}^3 \ell^m \mathbf{1}_k(m)]^{\frac{2}{\sigma-1}} w_t^2}{2\theta}. \end{aligned}$$

From the expression above, it is straightforward to see that when $\sigma = 3$, the death of a non-productive member with mass ℓ^m reduces $u(n_k)$ by ℓ^m fraction.

C Blinder-Oaxaca Decomposition

We use two-way Blinder-Oaxaca decomposition to understand the driving forces behind the expected number of children’s lives lost per COVID-19 fatality averted across country groups. This exercise divides the entire sample into two groups, with the LIC and the LMC in the first group and the UMC and HIC in the second. We include the semi-elasticity of child mortality with respect to income ($\nu(1)$), the population age distribution (ℓ_1 and ℓ_3), hospital capacity (κ), and the calibrated transmission parameters (π_{I1} , π_{I2} , and π_{I3}) on the RHS of the decomposition. Table C.1 reports the results of the decomposition exercise.

Table C.1: Blinder-Oaxaca Decomposition

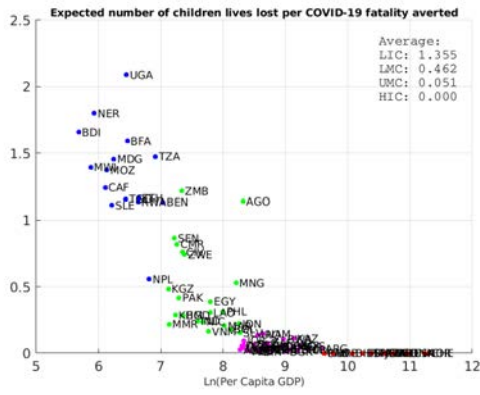
	Optimal Lockdown			Criteria-Based Lockdown		
	Overall	Explained	Fraction	Overall	Explained	Fraction
LIC + LMC	0.204 (0.021)		1.061 (0.121)			
UMC + HIC	0.010 (0.002)		0.039 (0.007)			
Difference	0.194 (0.021)		1.021 (0.122)			
Explained	0.283 (0.051)		1.659 (0.208)			
Unexplained	-0.089 (0.042)		-0.638 (0.164)			
Semi-Elasticity		0.226 (0.060)	0.798	1.333 (0.240)	0.803	
Population Share, 0-14		0.097 (0.031)	0.343	0.477 (0.172)	0.288	
Population Share, 65+		-0.015 (0.023)	-0.053	-0.047 (0.126)	-0.028	
Hospital Beds per 1000		-0.002 (0.003)	-0.007	-0.024 (0.020)	-0.014	
π_{I1}		-0.001 (0.011)	-0.004	0.032 (0.038)	0.019	
π_{I2}		0.009 (0.006)	0.032	0.061 (0.034)	0.037	
π_{I3}		-0.033 (0.014)	-0.117	-0.173 (0.059)	-0.104	
Constant						
N	85			85		

Note: this table reports the two-way Blinder-Oaxaca decomposition of the expected number of children lives lost per COVID-19 fatality averted by country groups. The first group is the low-income countries (LIC) and the lower-middle-income countries (LMC); the second group is the upper-middle-income countries (UMC) and the high-income countries (HIC).

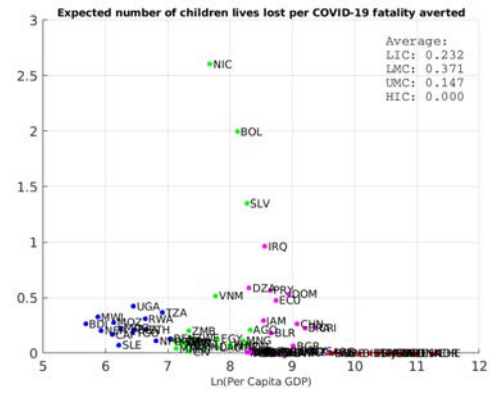
The columns “overall” reports the differences in means across country groups and the overall explanatory power of the RHS variables. In the detailed decomposition, it is clear that the income factors (the semi-elasticity) are by far the most prominent force, explaining

between 63.3 to 81.2% of the between-group differences. The age-structure, especially the population share of children between 0 and 14, explains most of the remaining variations. The hospital capacity has little power in driving variations across country groups.

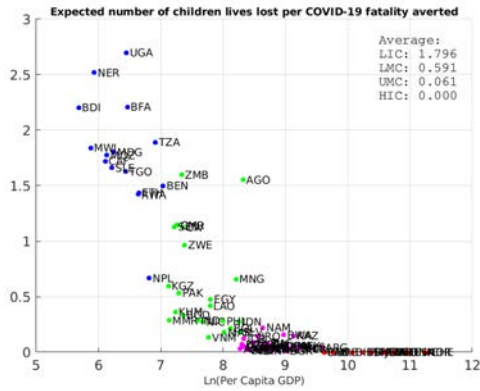
D Robustness



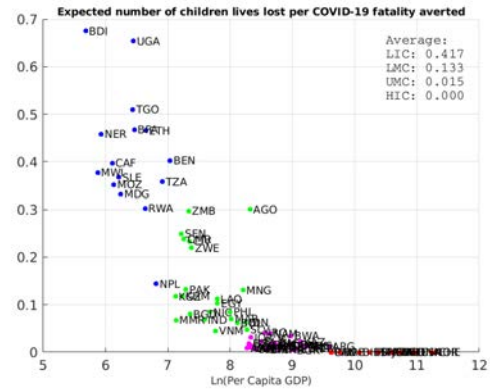
(a) criteria-based lockdown, $\sigma = 1.01$



(b) optimal lockdown, $\sigma = 1.01$



(c) criteria-based lockdown, $\sigma = 5$



(d) optimal lockdown, $\sigma = 5$

Figure D.1: Alternative values of σ